

Learning Objectives

- Ion formation under ambient conditions
- Interfaces for ambient desorption/ionization-mass spectrometry
- Screening techniques for rapid quality control and safety applications
- Real time examination of samples during physical manipulation

13.1 Concept of Ambient Desorption/Ionization

All methods for the generation of ions for mass spectrometry described up to this point require the analyte for ionization to be presented either directly under high vacuum (EI, CI, FI, FD) or contained in a sort of solution from which ions are to be extracted into or generated in the gas phase (FAB, LDI, MALDI). Even the atmospheric pressure ionization techniques employ processes that create ions from dilute (solid) solutions of the sample (ESI, APCI, APPI, AP-MALDI). This chapter deals with the manifold methods and interfaces which are allowing to overcome these limitations, and which have been developing at a breathtaking pace during the last decade.

Desorption electrospray ionization (DESI) [1] was introduced at the end of 2004. The novel feature of DESI is that it allows instantaneous mass spectral analysis without sample preparation or sample pretreatment. Furthermore, the object to be analyzed is handled at atmospheric pressure, i.e., in a freely accessible open space in front of the atmospheric pressure interface [2]. Soon after in 2005, *direct analysis in real time* (DART) followed [3].

The obvious potential of both DESI and DART in high-throughput applications quickly led to the development of some “derivatives” with the intention to broaden the field of applications or to adapt the underlying methodology to specific

analytical needs. DESI and DART are thus the pioneers of numerous *ambient desorption/ionization* (ADI) techniques – more than thirty of which have been published since then [4]. The unifying feature of all these, of course, is the presentation of the sample under ambient conditions and without sample pretreatment. The term *ambient mass spectrometry* has thus become widely used for this group of methods [4–7]. Both terms, *ambient MS* and *ambient desorption/ionization* (ADI) are currently being used. In all these methods analyte molecules are being “wiped off” from the samples by exposing their surfaces to some ionizing gas or aerosol [8].

The nice thing about ambient MS is that it allows for the examination of untreated samples or entire objects in the open environment while maintaining sample integrity [9]. Classical atmospheric pressure ionization (API) techniques, in contrast, require a sample to be dissolved or extracted from an object or an aliquot thereof. While in ambient MS, an object is simply positioned at the entrance of a mass spectrometer and molecules released from the sample (not necessarily the entire sample) are being ionized and transferred into the mass analyzer [7]. This means that sampling is now part of the process [8]. The beauty of ambient MS is that a sample only needs to be exposed to an ionizing fluid medium under ambient conditions (Fig. 13.1).

Plenty of methods

In this chapter, we are not looking at a single ionization method but at a group of techniques that share the feature of ambient desorption/ionization. The goal of subjecting an object, essentially its surface, to immediate mass spectral analysis by simply exposing it to some sort of ion source can be achieved in numerous ways. Approaches to do so are based on ESI, APCI, APPI, combinations thereof with laser desorption, and various electrical discharges to create ionizing plasmas as employed in DART, for example.

Now, the repertoire of ADI methods includes variations of the DESI theme such as *desorption sonic spray ionization* (DeSSI) [10], later renamed *easy sonic spray ionization* (EASI) [11] or *extractive electrospray ionization* (EESI) [12, 13]. Then, there are the DESI analogs of APCI and APPI, i.e., *desorption atmospheric pressure chemical ionization* (DAPCI) [14, 15] and *desorption atmospheric pressure photoionization* (DAPPI) [16].

Analyte ions withdrawn from the sample are transported through air into the mass analyzer via a standard API interface. DESI, DART, and those numerous related methods enable the detection of surface materials like waxes, alkaloids, flavorants, or pesticides from plants as well as explosives, pharmaceuticals, or drugs of abuse from luggage or banknotes. These and many more analytical applications are readily accessible – even without harm to living organisms [17]. This simplified sample pretreatment is key to the success of ambient MS. In ambient MS, samples are accessible to observation and may even be subjected to

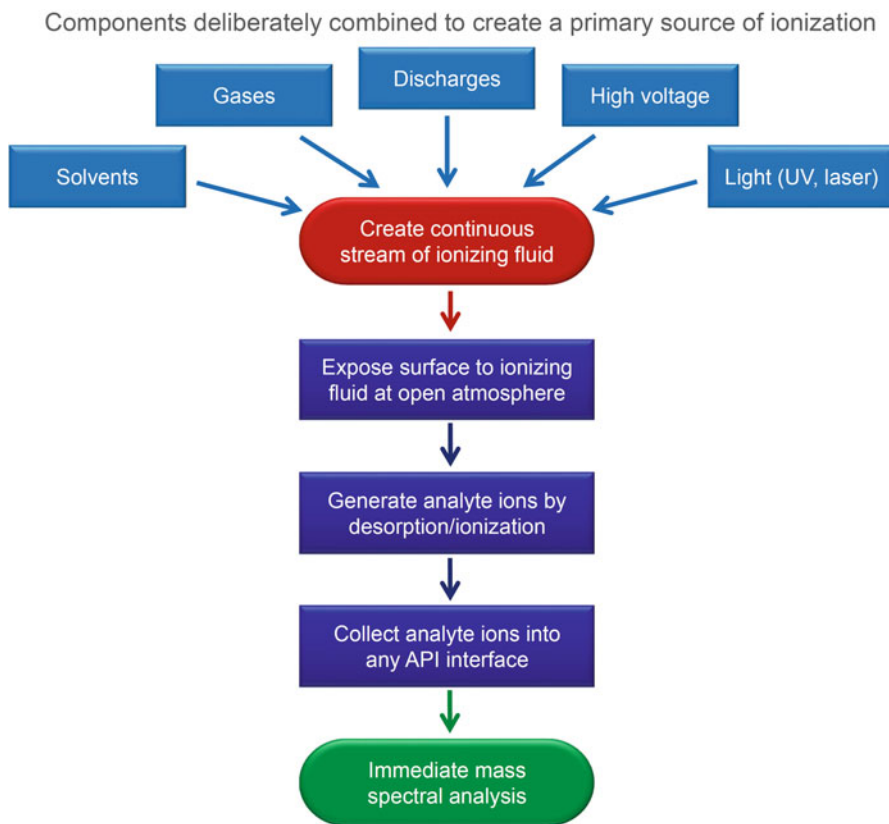


Fig. 13.1 Concept of ambient desorption/ionization mass spectrometry

some kind of processing, either mechanical manipulations or chemical treatments, while mass spectra are continuously being measured. Even a portable ion trap mass spectrometer for use with commercial DESI and DART ion sources has been designed [18].

Grounded euphoria

Although the features of DESI, DART, and many other ADI methods are in many ways superior and “revolutionary”, one should be aware of intrinsic limitations. The detection of a compound largely depends on the matrix, e.g., whether it is *on* or eventually *in* skin, fruit, bark, stone etc. This also results in a limited quantification potential. However, also no other single ionization method, especially when used under just one set of conditions, can deliver ions of all constituents of a complex sample. Nonetheless, DESI, DART, and related methods can deliver a wealth of chemical information with unprecedented ease.

13.2 Desorption Electrospray Ionization

Desorption electrospray ionization (DESI) [1, 19] is applicable to solids, liquid samples, frozen solutions, and to loosely surface-bound species like adsorbed gases. It can detect low-molecular-weight organic compounds as well as comparatively large biomolecules [1, 19–21]. The material presented to DESI may be a single compound suitably prepared on a sample target analogous to LDI or it can be a complex biological material like tissue, blood, whole leaves, or fruit [22].

13.2.1 Experimental Setup for DESI

DESI is derived from electrospray ionization (ESI, Chap. 12) [23, 24] in that it employs an electrically charged aerosol that is created by pneumatically-assisted electrospray of a solvent containing some electrolyte at low concentration [1, 19]. In a standard ESI experiment the spray capillary is set to high voltage in respect to a counter electrode that is essentially represented by the atmospheric pressure entrance of the interface. Sample ions are already contained in the solution that is supplied to the sprayer. In DESI, the spray capillary is shifted away from the orifice of the API interface and only a solvent or solvent mixture is sprayed under strong pneumatic assistance onto a surface at an impact angle α , typically close to 45° . The distance between spray capillary and object is adjusted to a few millimeters and the entrance of the API interface is aligned at a similar angle and distance. Thus, sprayer, object, and orifice form a compact V-alignment. Driven by the high-velocity gas stream, the highly charged aerosol droplets receive sufficient kinetic energy to be forced onto the sample surface even while an electrostatic charge is building up there. The resulting interaction may cause surface coverage with a thin liquid film, and thus, dissolve and take up analyte ions. A surface analyzed by DESI gets “wet”. This way, the solvent can also extract analytes from the object. The final release of isolated gas phase ions follows the same pathways as in ESI. Like ESI, DESI is capable of analyzing compounds from very low to high mass range while preserving the intact molecules [4].

Local electrostatic charging and the reflected gas stream now act in concert and transport analyte ions away from the surface at an angle β (Fig. 13.2). A nearby sampling orifice may then inhale a portion of the mist in the same way as it normally would do when the sample is already admixed to the solvent system. To bridge the gap between the sampling area and the entrance into the interface, a transfer line or extension tube is mounted in front of the orifice. This tube, e.g., 3 mm o.d. stainless steel, simplifies handling and particularly accessibility of the sample and also improves desolvation of the ions, probably due to different droplet sizes as compared to standard ESI conditions [1, 2]. DESI practice has shown that interfaces with a heated transfer capillary are superior to those employing a counter-current desolvation gas and corresponding modifications have been suggested [25].

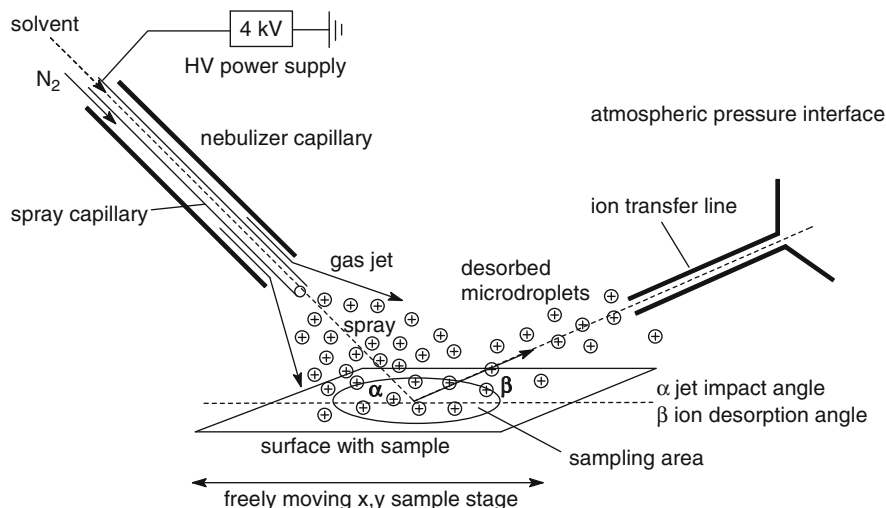


Fig. 13.2 Schematic of a DESI interface. A jet of gas and charged microdroplets is created by means of a standard pneumatic ESI sprayer and directed onto a sample surface at angle α . As a result, charged microdroplets containing ions of the surface material are created and transported away due to the action of the reflected gas stream and electric repulsion at angle β . A portion of the “secondary ESI spray” may be taken up by the atmospheric pressure interface of the mass spectrometer. Although at the expense of optimum sensitivity, an extended ion transfer line is normally employed to bridge the gap from surface to interface sampling orifice [1, 2]

Early on, commercial DESI sources have become available and have meanwhile reached a level of maturity. They feature ESI sprayers adjustable in both angle and distance towards sample plates that can be operated under data system control (Fig. 13.3).

Custom-built DESI source?

In principle, any mass spectrometer equipped with an ESI source can be modified for DESI operation by mounting the sprayer on an adjustable frame and placing a x,y-movable sample stage between sprayer and entrance of the interface [26]. For safety, a G Ω -resistor should be welded in the high-voltage supply cord. However, for successful analytical application, only sensitive modern instruments are suitable.

13.2.2 Parameters for DESI Operation

Obviously, DESI introduces new parameters to the ESI experiment. In particular, the velocity of the spray gas (represented by the supply pressure), the sprayer-to-surface and sampling orifice-to-surface distances, and the angles of impact and



Fig. 13.3 A commercial DESI ion source. This one here is the Prosolia Omni Spray 2D source coupled to a Thermo Fisher LTQ mass spectrometer. The surface shown is a 96-spot Omni Slide HC having the standard microtiter plate dimensions. Note the extended desolvation capillary and the adjustable sprayer (Courtesy Prosolia, Inc., Indianapolis, IN USA)

desorption are contributing to the affectivity of ion generation and subsequent uptake into the mass spectrometer. Accordingly, these parameters need to be carefully optimized for any DESI application as they exhibit rather wide variations (Table 13.1) [2, 22]. It has also been found that optimum settings differ between API interfaces with counter-current drying gas and those employing the heated desolvation capillary design [27]. The transit of charged particles from the sample surface into the ion transfer line of the interface is determined, among others, by the dragging action of the mass analyzer's vacuum.

Additional parameters associated with DESI are the electrical conductivity, the chemical composition, and the texture of the sample surface. Neutralization of the droplets landing at the surface must be avoided to maintain continuous release of charged particles from the surface. Conductive sample supports need to be either isolated or floated at a potential equal to or slightly lower than the spray voltage. The electrostatic properties of the surface are also relevant for an insulator, because the signal stability depends on its preferred polarity. A highly electronegative polymer like PTFE, for example, yields better signal stability in negative-ion mode, whereas PMMA performs better in positive-ion mode. The chemical composition of the surface can affect crystallization of the analyte, and thus, as observed in MALDI preparations, lead to the occurrence of "sweet spots". Therefore, high affinity of analyte molecules to the surface needs to be avoided as it is detrimental for the release of analyte. Finally, the surface texture plays a role. The use of HF etched glass slides as DESI substrates instead of untreated ones delivered a dramatic increase in signal stability and eliminated "sweet spot" effects. Generally, rough surfaces like paper or textiles give superior sensitivity [2].

Optimization of DESI conditions Examinations have been carried out on the dependence of the signal intensity of the $[M+3H]^{3+}$ ion of melittin on basic

Table 13.1 Typical parameters for DESI

Parameter	Range of useful settings
Solvent flow rate	3–5 $\mu\text{l min}^{-1}$
Nebulizer gas pressure	8–12 bar
Spray voltage	2–6 kV
Sprayer-to-surface distance	1–5 mm
Sprayer-to-surface angle	30–70°
Surface-to-desolvation capillary distance	1–5 mm
Surface-to-desolvation capillary angle	10–30°
Temperature of desolvation capillary	200–300 °C

experimental DESI parameters such as spray impact angle, spray high voltage, nebulizing gas inlet pressure, and solvent flow rate. Methanol : water = 1:1 was sprayed onto a sample of 10 ng melittin deposited on a PMMA surface at fixed spray tip-to-surface distance of 1 mm. While one parameter was varied, the others were kept constant at about their average value. The results reveal optimum conditions for each parameter that are rather typical for DESI and, as far a flow rate and spray high voltage are concerned, also for ESI (Fig. 13.4) [2].

DESI parameters can be grouped in a compound class-specific manner. It was found that proteins, for example, yield stronger signals when the spray is pointed onto the sample from close to vertical at about 1 mm distance while small molecules such as caffeine work best at an angle around 45° and several millimeters distance from the spray needle (Fig. 13.5) [2].

13.2.3 Mechanisms of Ion Formation in DESI

In DESI an electrospray plume of electrolytic solvent is usually generated by applying a potential of several kilovolts to an electrolytic solution under (strong) pneumatic assistance [2]. The mist comprising charged microdroplets, ionic clusters, and gas phase solvent ions is directed onto the sample surface. Therefore, the physical state of the sample distinguishes DESI from ESI. In this respect, DESI shows some phenomenological relationships to desorption ionization, because methods such as plasma desorption (PD), (matrix-assisted) laser desorption ionization ((MA)LDI), as well as fast atom bombardment (FAB) and its inorganic variant secondary ion mass spectrometry (SIMS, Sect. 15.6) all involve the impact of projectiles on condensed phase samples. Depending on the method, these projectiles are either photons, energetic atoms, or ions. In contrast to those desorption methods, DESI is performed in the ambient atmosphere, and therefore, the projectiles in DESI can only possess low kinetic energies.

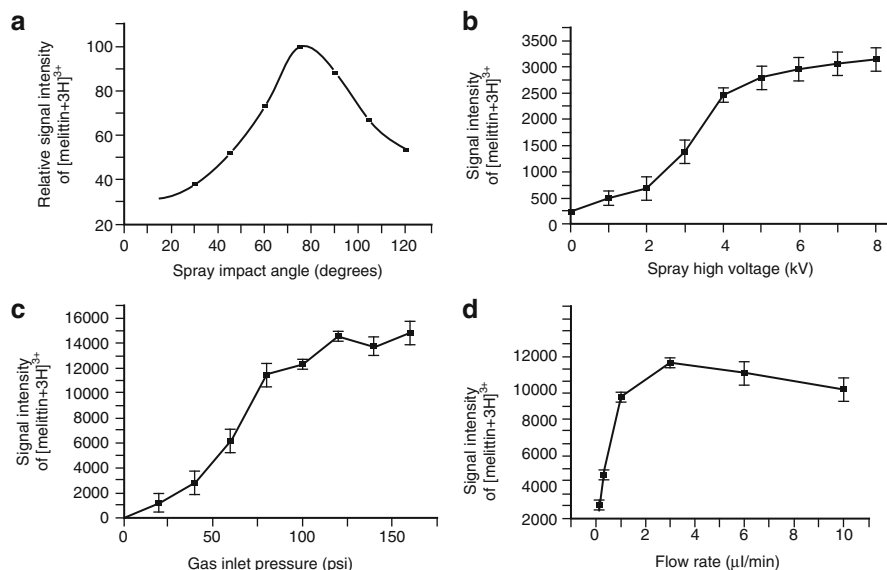


Fig. 13.4 Influence of experimental parameters on the intensity of the $[M+3H]^{3+}$ ion of melittin: (a) spray impact angle, (b) spray high voltage, (c) nebulizing gas pressure (14.5 psi \approx 1 bar), (d) solvent flow rate (Reprinted from Ref. [2] with permission. © John Wiley & Sons, Ltd. 2005)

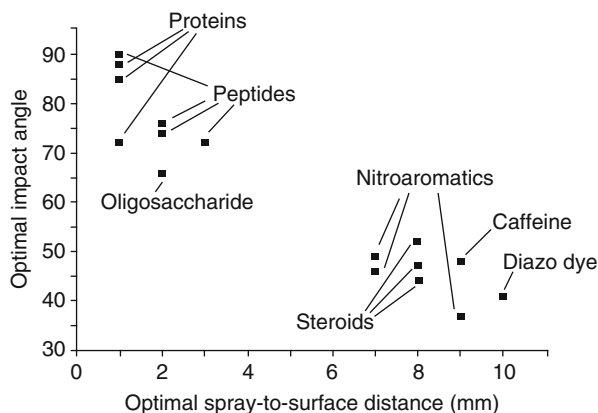


Fig. 13.5 Compound class-specific optima of spray impact angle and spray needle distance to surface. The *upper left* group of analytes would preferably be analyzed by ESI whereas the *lower right* group would rather demand for APCI (cf. Sect. 7.8) (Reprinted from Ref. [2] with permission. © John Wiley & Sons, Ltd. 2005)

Three processes of ion formation have been proposed for DESI [21]. Depending on the conditions and applied solvent-analyte pair, one of the following will predominate:

Droplet pickup *Droplet pickup* involves impact of electro sprayed droplets on the surface followed by dissolution of the analyte from the surface into the droplets. The droplets are again released from the surface and subsequent evaporation of the solvent and Coulomb fission generates ions by processes analogous to conventional ESI. The droplet pickup mechanism accounts for the similarity of DESI spectra with those of standard ESI in case of proteins. Interestingly, peptide ions can be observed even when the target and the sprayer are held at equal electrical potential. This has been attributed to the effect that offspring droplets will emerge mainly from the edges of a spreading primary droplet. In this case, charged droplet formation would essentially occur by electrospray driven by the potential between the edges and the extended desolvation capillary.

Condensed phase charge transfer When gaseous ions delivered by the electrospray interact with the analyte surface this can result in *condensed phase charge transfer*. The desorption of the analyte ions from the surface is then thought to occur by a type of *chemical sputtering*. (Chemical sputtering is a process in which ion bombardment induces chemical reactions that finally lead to the formation of volatile erosion products [28].) This way, ions can be formed by transfer of electrons, protons, or other small ions from the impacting microdroplet to the surface bearing the analyte. A surface charge builds up and the momentum delivered from the impact event may then suffice to effect direct release of analyte ions from the surface. This proceeds at very low impact energy if the reactions are exothermic, while somewhat higher energies (adjusted via gas pressure) are required to achieve lift-off in case of endothermic reactions.

Gas phase charge transfer Ion formation after volatilization or desorption of neutral species from the surface into the gas phase can lead to *gas phase charge transfer*. Ionization then proceeds via proton/electron transfer or other ion–molecule reactions at atmospheric pressure. Indeed, the assumption of ion–molecule reactions, eventually purely in the gas phase above the sample, has led to the development of an DAPCI source (Sect. 13.3), in the first place to prove this mechanism of ion formation [14]. The solvent pH can be used to positively affect the vapor pressure of the analyte, e.g., the vapor pressure of volatile plant alkaloids is increased by addition of a base.

13.2.4 Analytical Features of DESI

DESI can serve for the identification of natural products in plant material [1, 2, 22], of lipids in animal tissue [27, 29], for high-throughput analyses of pharmaceutical preparations [20], and for drug metabolite identification or even quantitation in blood and other biological fluids [2, 25], as well as for the direct monitoring of biological tissue for biomarkers and in vivo analysis [17, 27, 29]. DESI is applicable to the analysis of proteins, carbohydrates, and oligonucleotides [2], as well as small organic molecules. Potential DESI applications are also in forensics and

public safety such as the detection of explosives, toxic compounds, and chemical warfare agents on a variety of common surfaces, e.g., paper, plastics, cloth or luggage [21, 30]. Plastic explosives, i.e., formulated explosive mixtures, can also be analyzed [17, 21, 30]. Even the transfer of ion-loaded gas from the sample to the API source through an up to three-meter-long stainless-steel tubing, termed non-proximate sampling, has been demonstrated [31].

The limit of detection for small peptides is in the order of 1 pg absolute or $<0.1 \text{ pg mm}^{-2}$, for proteins in the order of $<1 \text{ ng absolute}$ or $<0.1 \text{ ng mm}^{-2}$; small molecules such as pharmaceuticals and explosives are detectable in the range of 10–100 pg absolute or $1\text{--}10 \text{ pg mm}^{-2}$ [2, 17]. These numbers indicate a footprint of about 10 mm^2 roughly corresponding to a circular spot of 3 mm in diameter. Smaller footprints can be realized – sample and sensitivity of the instrument permitting. The number of DESI papers is steadily growing. A few representative examples of DESI applications are compiled below.

Pharmaceuticals The negative-ion DESI mass spectrum of the over-the-counter drug acetylsalicylic acid (aspirin) was measured with a home-built DESI source attached to a seasoned triple quadrupole instrument (Fig. 13.6). The sample was presented on paper to a methanol spray. Whereas this sample even allowed tandem mass spectra of the $[\text{M}-\text{H}]^-$ ion, m/z 179, to be readily obtained, other samples were beyond the instrument's sensitivity limits [26].

Poisonous plants Plant alkaloids can be identified from DESI mass spectra of seeds, leaves, flowers, or roots. Here seeds of deadly nightshade (*Atropa belladonna*) were subjected to DESI for the identification of their principal alkaloids

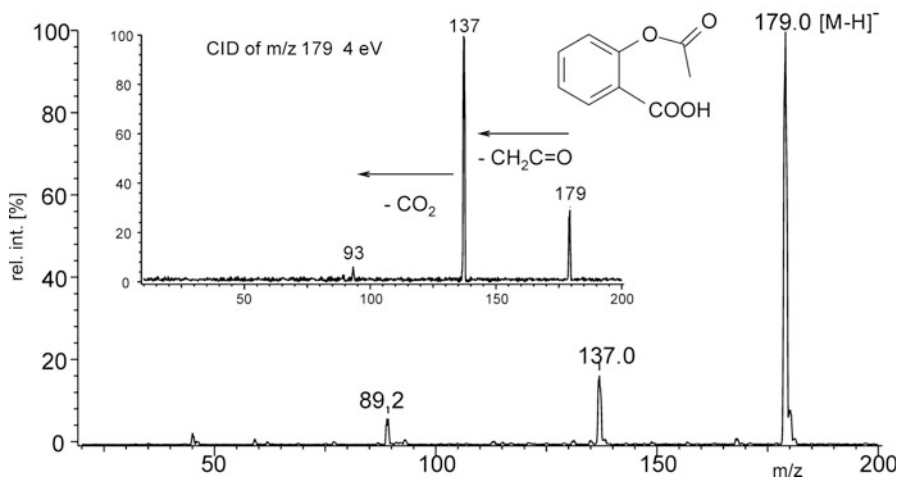


Fig. 13.6 Testing of a home-built DESI source. DESI mass spectrum of acetylsalicylic acid from paper analyzed by negative-ion DESI using methanol spray. The inset shows the tandem mass spectrum of the deprotonated molecule

atropine and scopolamine (Fig. 13.7) [22]. (Atropine is the name of the racemic mixture of (*R*)- and (*S*)-hyoscyamine. It is a tropane alkaloid also extracted from jimsonweed (*Datura stramonium*), mandrake (*Mandragora officinarum*) among other plants of the Solanaceae family.) The inset in Fig. 13.7 shows tandem mass spectra of the ions at m/z 290 and 304, thereby confirming them as corresponding to protonated hyoscyamine and scopolamine, respectively. The confirmation of the ion at m/z 304 as $[M+H]^+$ ion of scopolamine was obtained by comparing the tandem mass spectrum with that of the standard alkaloid.

Animal tissue Mouse liver sections were analyzed by DESI-FT-ICR-MS. The spectra of the tissue samples exhibited strong signals for phospholipids and lysophospholipids that were detected either as $[M+H]^+$, $[M+Na]^+$, or $[M+K]^+$ ions. The mass accuracy of generally 1 ppm of the FT-ICR instrument allowed for assigning unique molecular formulas to most signals (Fig. 13.8) [27].

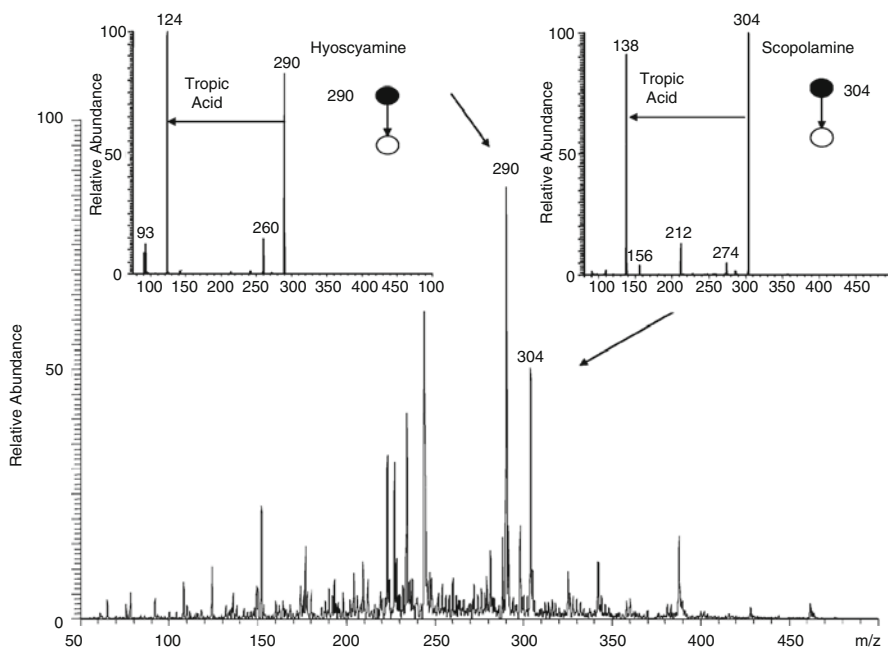


Fig. 13.7 DESI mass spectrum of *Atropa belladonna* seeds using methanol : water = 1:1 as spray solvent. The insets show tandem mass spectra of the protonated alkaloids hyoscyamine, m/z 290 and scopolamine, m/z 304. Both protonated alkaloids have the characteristic loss of tropic acid, 166 u, in common (Reprinted from Ref. [22] with permission. © The Royal Society of Chemistry, 2005)

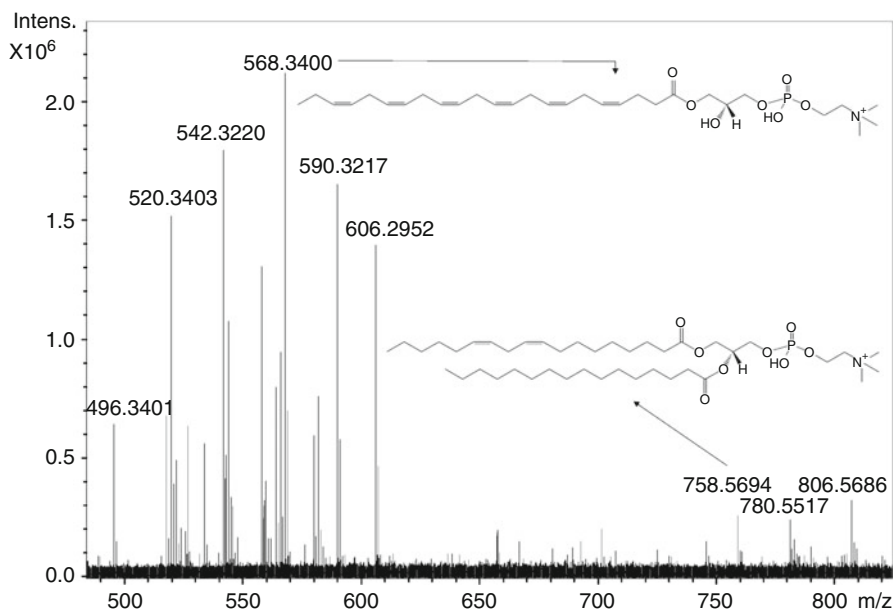


Fig. 13.8 Lipid profile of murine liver tissue sections as acquired by DESI-FT-ICR-MS using methanol : water = 1:1 (v/v) with 1% acetic acid as spray solvent (Reproduced from Ref. [27] with permission. © John Wiley & Sons, Ltd., 2008)

DESI of TLC plates Thin layer chromatography (TLC) plates were first analyzed by DESI in the van Berkel group [32]. The sprayer was positioned about 4 mm from the curtain plate of the mass spectrometer at a 50° angle relative to the TLC plate surface. The TLC plates were cut to align the sample bands with the DESI plume. Methanol was sprayed at about 5 $\mu\text{l min}^{-1}$ while a *x-y-z* robotic platform and control software were used to move the TLC plate relative to the stationary DESI emitter at about 50 $\mu\text{m min}^{-1}$. The position of the TLC plate relative to the sprayer was monitored with a camera, the image of which was output to a PC so as to correlate staining, position, and DESI spectral data (Fig. 13.9).

Scrutinize the spectra

Although it appears that the results of DESI analyses (or of any other ADI technique) are almost instantaneously available, DESI spectra tend to require more thorough examination than standard ESI spectra in order to draw the right analytical conclusions.

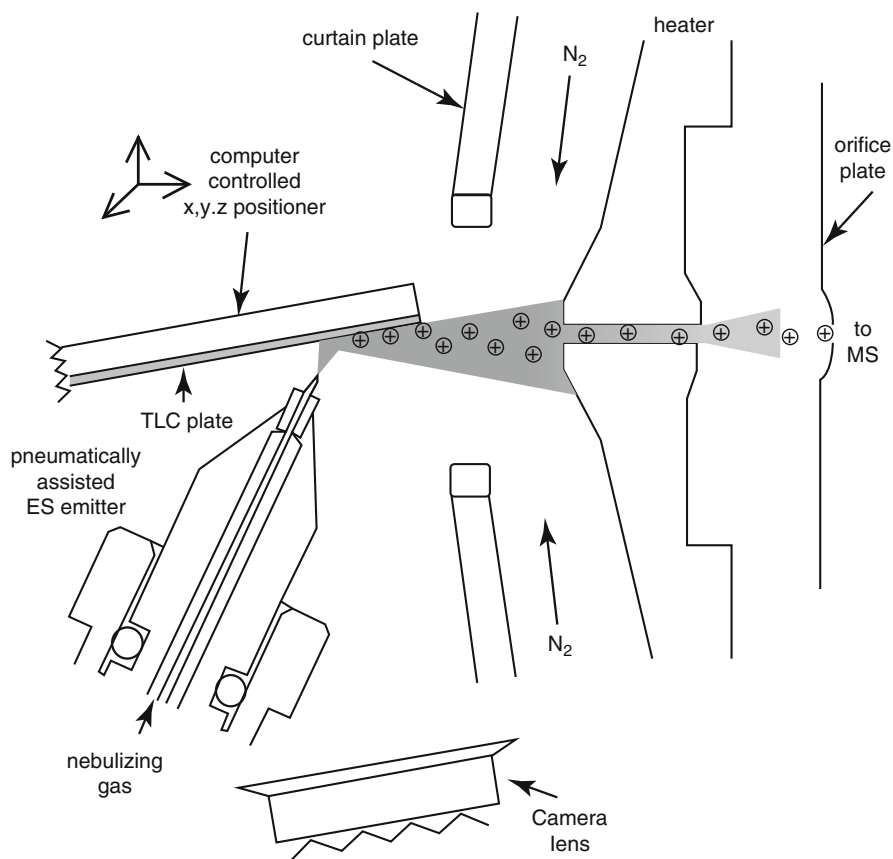


Fig. 13.9 Fully computer-controlled TLC-DESI unit attached to an ESI interface using the curtain gas design (Reprinted with permission from Ref. [32]. © The American Chemical Society, 2005)

13.3 Desorption Atmospheric Pressure Chemical Ionization

The first report on *desorption atmospheric pressure chemical ionization* (DAPCI) appeared in a paper on the analysis of nitroaromatic explosives by negative-ion DESI [14]. These molecules all possess high electron affinities and thus they are prone to electron capture and deprotonation. From the positive effect of the DAPCI mode of operation for their detection, it was inferred that a chemical ionization mechanism should be effective if analytes are volatilized in the course of DESI analysis. So the main difference between DESI and DAPCI is the substitution of the charged solvent mist by a (hot) solvent vapor and the application of a corona discharge as the initial source of electric charge in DAPCI [21]. As usual in APCI, the corona discharge is created by applying a high DC voltage (3–6 kV) to

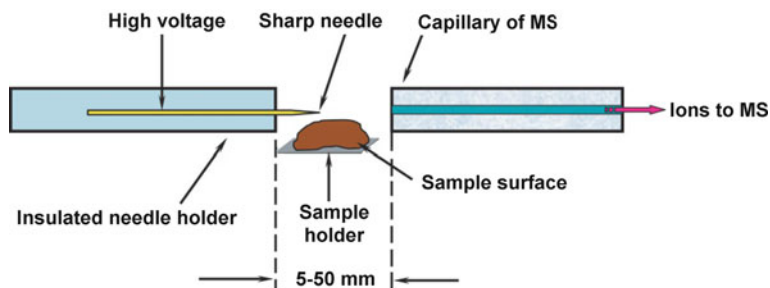


Fig. 13.10 Schematic of a DAPCI source for operation with moist ambient air as reagent gas. The sharp needle discharge electrode is coaxially centered in a capillary of 3 mm i.d. delivering humidified nitrogen gas if the ambient air is below 20% relative humidity (Adapted from Ref. [33] with permission. © John Wiley & Sons, Ltd., 2007)

a tapered tip stainless steel needle. Reactant ions are created in the solvent vapor upon passing the discharge. Then, the ionized gas streams onto the surface to be analyzed. Obviously, the droplet-pickup mechanism (Sect. 13.2.3) is precluded in DAPCI, while charge transfer to the surface and gas phase ionization of the analyte present the two possible mechanisms of ion formation [31].

It has been shown that addition of solvents can be avoided if the moisture of the ambient air is sufficient to generate H_3O^+ reagent ions [15, 33]. The setup for DAPCI (using ambient air only) is shown in Fig. 13.10. A comparison of spectra of Proctosedyl, an ointment containing cinchocaine ($M_r = 343$ u) and hydrocortisone ($M_r = 362$ u), as obtained by DESI, DAPCI with ambient air, and DAPCI with solvent is presented in Fig. 13.11.

Applications of DAPCI include the comparative analysis of different teas such as green tea, oolong, and jasmine tea by their chemical fingerprints [33, 34] and the direct rapid analysis of melamine and cyanuric acid in milk products delivering detection limits of 1–20 pg melamine mm^{-2} [35]. Furthermore, DAPCI has been successfully employed for the detection of peroxide explosives [30] or of illicit ingredients in food such as sudan red dyes in tomato sauce [33]. Analogous to DESI, DAPCI analyses can be performed with remote sampling [31].

13.4 Desorption Atmospheric Pressure Photoionization

DESI works best with polar analytes that are easy to protonate or deprotonate, although analytes of low polarity are accessible to a certain extent. This was the rationale for developing DAPCI. In order to improve the efficiency of ambient MS in the regime of low-polarity compounds even further, *desorption atmospheric pressure photoionization* (DAPPI) has been developed. DAPPI represents the adaptation of APPI for the ambient analysis of surfaces analogous to the conversion of APCI to DAPCI.

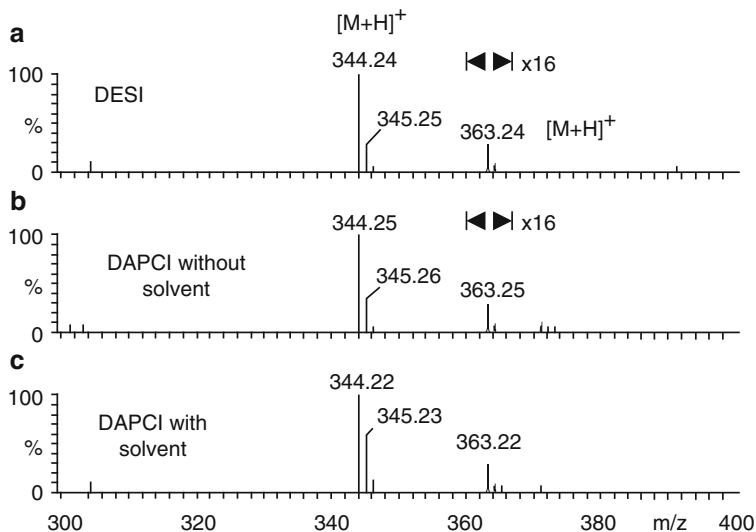


Fig. 13.11 Comparison of DESI, solvent-free DAPCI and DAPCI of Proctosedyl ointment. (a) Positive-ion DESI spectrum with the intensity of m/z 363, protonated hydrocortisone, 16-fold expanded to show the low-abundant ion. (b) Positive-ion DAPCI spectrum of the ointment obtained without solvent and same expansion as above. (c) Positive-ion DAPCI spectrum obtained with solvent (Reproduced from Ref. [15] with permission. © John Wiley & Sons, Ltd., 2006)

In DAPPI, a heated jet of solvent vapor and nebulizer gas desorbs solid analytes from the surface. Using a microchip nebulizer turned out to be advantageous for handling and for highly responsive temperature control of the gas. The microchip nebulizer is a small glass device for mixing gas and solvent flow (dopant) and for heating the fluid medium during its passage along a platinum wire (Fig. 13.12) [16]. A krypton discharge lamp is directed toward the sample so as to irradiate the vapor phase immediately above the surface with UV photons of 10 eV where ionization of the analyte occurs. Like DESI and DAPCI, DAPPI uses a standard API interface to collect the ions [16, 36].

The mechanism of ion generation in DAPPI has been proposed to be a combination of thermal and chemical processes. After thermal desorption of the analytes from the surface they can be photoionized in the gas phase. However, analytes with no UV chromophore may only be ionized by ion–molecule reactions with dopant ions. Dopant molecular ions, D^+ , as formed from toluene for example, may promote charge exchange, while protonated dopant molecules, $[D+H]^+$, will yield $[M+H]^+$ ions. Acidic analytes can undergo deprotonation, while electronegative molecules are prone to anion addition or electron capture [36]. (The rules governing these processes have already been dealt with in Chap. 7). The factors influencing the desorption and ionization in DAPPI such as the microfluidic jet impinging geometry, the thermal characteristics of the surfaces subjected to DAPPI, as well as chemical aspects like spray solvent have been examined for both positive- and negative-ion mode [36].

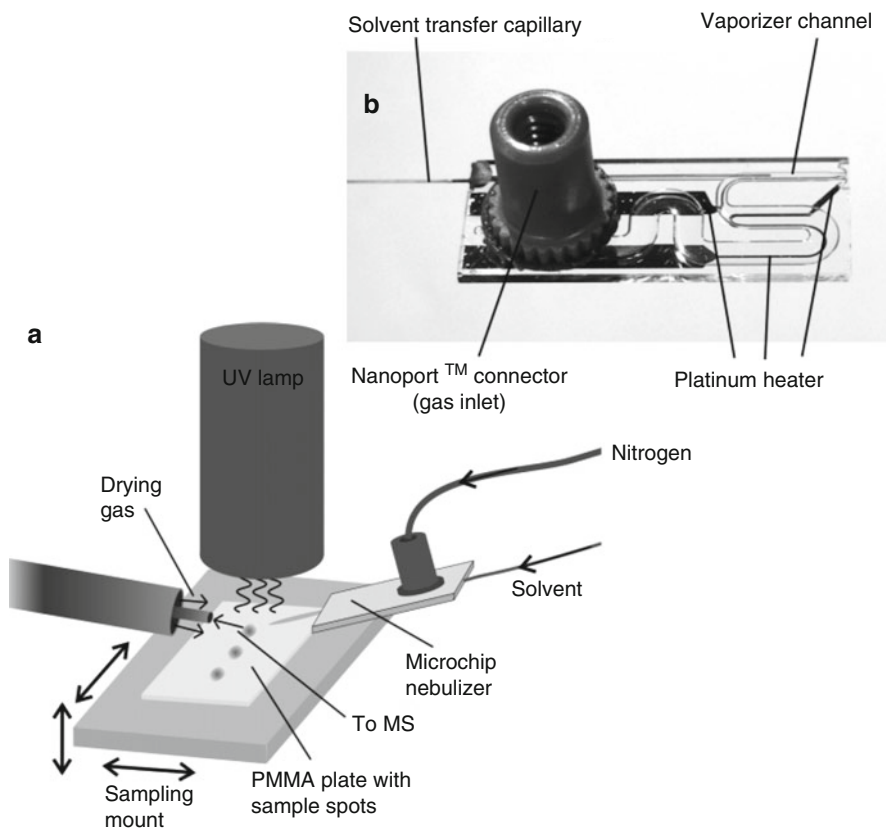


Fig. 13.12 Schematic of (a) the DAPPI setup and (b) photograph of the microchip nebulizer. The small solvent flow is mixed with nitrogen gas and vaporized in the microchip nebulizer by resistive heating of the platinum wire. The krypton UV lamp irradiates the sample surface that is in contact with the hot reagent gas (Reproduced from Ref. [16] with permission. © The American Chemical Society, 2007)

DAPPI is capable of analyzing dried sample spots of compounds of different polarities from various surfaces, may serve for the direct analysis of pharmaceuticals and illicit drugs from tablets and other preparations (Fig. 13.13), and of many other applications [16, 36–38].

13.5 Other Methods Related to DESI

Variation of the DESI theme by changing the mode of sample supply opens up a large variety of partially awe-inspiring, partially slightly odd, but always interesting analytical applications. In some cases, even the term was not finally coined at the time of their first publication.

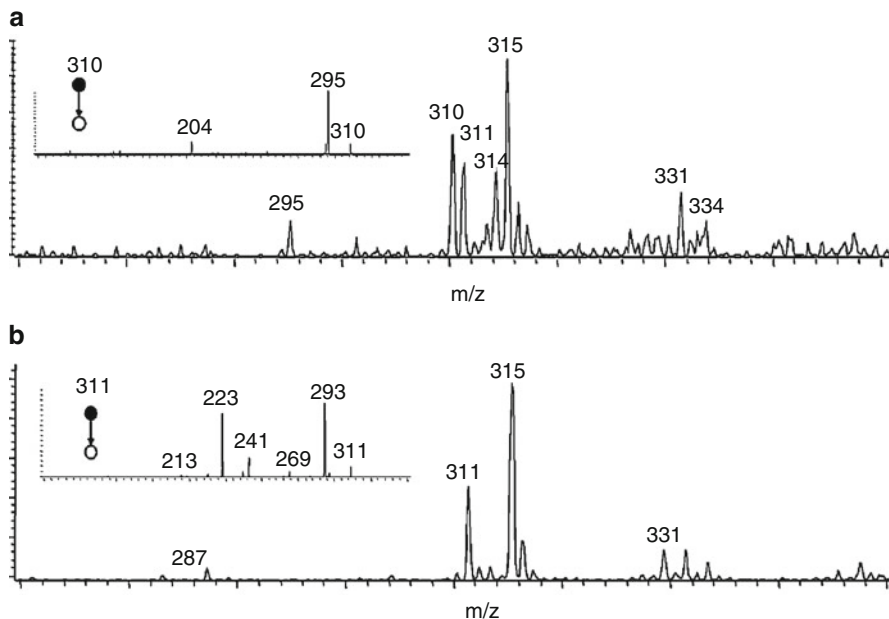


Fig. 13.13 Analysis of a hashish slab with DAPPI using toluene (a) and acetone (b) at flow rates of 2 ml min^{-1} as spray solvents. The insets show the tandem mass spectra of (a) the M^{++} ion of cannabinol and (b) the $[M+H]^+$ ion of cannabinol; the ions at m/z 314 and 315 are attributed to the respective ionic species of tetrahydrocannabinol (THC) (Reproduced from Ref. [38] with permission. © John Wiley Sons, Ltd., 2008)

13.5.1 Desorption Sonic Spray Ionization

In ESI an electrolytic solution is sprayed mainly by the action of an electric field inducing charge separation and subsequent disintegration of a bulk liquid into an electrostatically charged mist. A nebulizing gas flow at sonic speed coaxially to the liquid flow can also create a statistical imbalance of charges, i.e., a charge separation sufficient for the purpose of forming charged droplets. This is known as *sonic spray ionization* (SSI) [39–41]. The advantage of SSI is that it operates free of a high voltage and thus appears ideal for handling under ambient conditions [10]. An adaptation of SSI for ambient mass spectrometry was thus made and initially termed *desorption sonic spray ionization* (DeSSI) [10].

Naming

Soon after its introduction, DeSSI was renamed *easy ambient sonic-spray ionization* (EASI) [42], the superfluous inclusion of the adjective “easy” and the generation of a rather blatant acronym (EASI) seem to have driven this change.

DeSSI (or EASI) requires unusually high backpressure of ca. 30 bar to achieve the sonic velocity of the nebulizer gas stream resulting in a flow of about 3 l min^{-1} to dissipate the liquid flow of $20 \mu\text{l min}^{-1}$ methanol/water solution. The curtain gas pressure of the API interface is also set to a rather high value of 5 bar.

The method has shown to deliver good results for the fingerprinting of biodiesel fuel [43] and perfumes [42], for the analysis of fabric softeners and surfactants [44], coupling to membrane inlet systems (MIMS-DeSSI) [11], and to analyze components separated on TLC plates [45]. However, the method appears to exhibit low inter-system compatibility; in some laboratories high voltages were needed to obtain a signal.

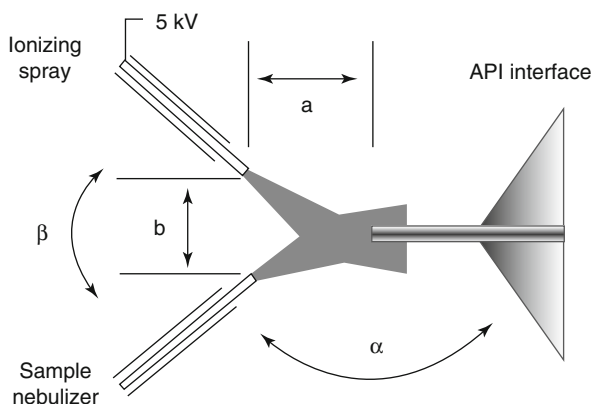
13.5.2 Extractive Electrospray Ionization

Analyte ions can also be efficiently generated when sample vapor or finely dispersed sample droplets transported by a carrier gas stream are admixed to the expanding electrospray plume. This technique, simple yet effective, has been introduced as *extractive electrospray ionization* (EESI) [46]. It utilizes two separate sprayers, one conventional ESI sprayer to provide the electrostatically charged mist and another to supply the sample vapor or mist (Fig. 13.14). While this approach is suggested for API interfaces with the heated transfer capillary design, the sample carrier stream may alternatively be passed into the desolvation gas of interfaces employing the heated curtain gas design (Fig. 13.15) [13, 47].

Instead of a separate sample sprayer, an ultrasonic nebulizer may also deliver a sample-containing aerosol, which is transported and admixed to the electrospray mist by action of a mild stream of nitrogen. As the droplets of both origins are “fused” inside a small housing enclosing the spray, this approach has been termed *fused-droplet electrospray ionization*, and thus, led to the somewhat confusing acronym FD-ESI [48, 49].

EESI has its strengths in headspace analytical applications; it has been employed to classify authentic perfumes and to detect counterfeit products from chemical

Fig. 13.14 Extractive electrospray ionization interface with two mixing sprays in front of a heated transfer capillary. The distances a and b and the angles α and β are adjusted as required for optimum signal intensity (Adapted from Ref. [46] with permission. © The Royal Society of Chemistry, 2006)



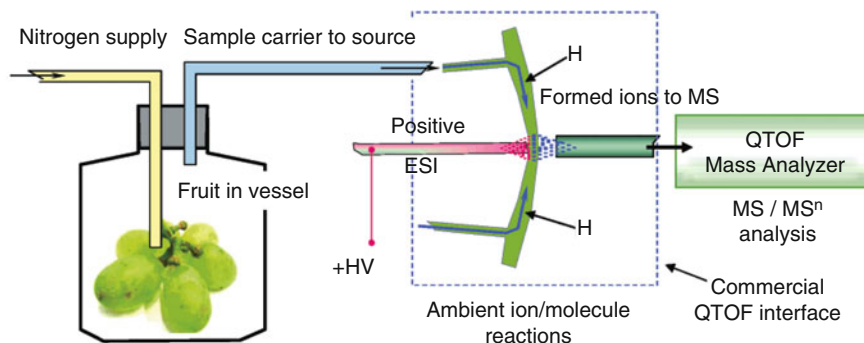


Fig. 13.15 Schematic of an EESI source where the sample carrier gas is fed into the curtain gas of the API interface. Here, the experiment is designed to determine the ripening of fruit from its headspace, i.e., odor (Adapted from Ref. [50] with permission. © The American Chemical Society, 2007)

fingerprints of the fragrances after their application on paper strips as usually performed for customer's testing [51]. It may serve for the rapid determination of the ripening of fruit via headspace analysis as pointed out in Fig. 13.15 [50], or to identify spoiled food, either vegetables or meat samples, even in the frozen state, by detection of typical degradation products or metabolites from bacterial growth [12, 47]. It is also possible to detect melamine in milk [52] (a sort of analysis one never would have assumed to be necessary until after the Olympic games in China in 2008). Finally, as the location of the extraction can be several meters away from the mass spectrometer, traces of toxic chemicals, explosives, or drugs on skin can be detected by EESI without any hazard to a person [13, 53].

13.5.3 Electrospray-Assisted Laser Desorption/Ionization

The technique of *electrospray-assisted laser desorption/ionization* (ELDI) combines two well-matured techniques of ionization for the benefit of improved analysis of samples under ambient conditions. The development of ELDI emanates from the fact that in (MA)LDI by far more neutrals than ions are released from the sample layer (Chap. 11) [54]. Consequently, post-ionization of laser-desorbed neutrals is promising and such methods have indeed been developed (cf. Refs. in [55]). The unique feature of ELDI is to laser-irradiate the sample in the ambient close to the ESI plume, wherein the neutrals are then ionized by ion–molecule reactions [55].

Standard conditions of ESI for ELDI involve a methanol : water = 1:1 mixture with 0.1% acetic acid sprayed at $3\text{--}5\ \mu\text{l min}^{-1}$ from a grounded needle as to pass closely over an also grounded sample support. The orifice of the API interfaces acting as the counter electrode is held at 4–5 kV negative voltage. The UV nitrogen

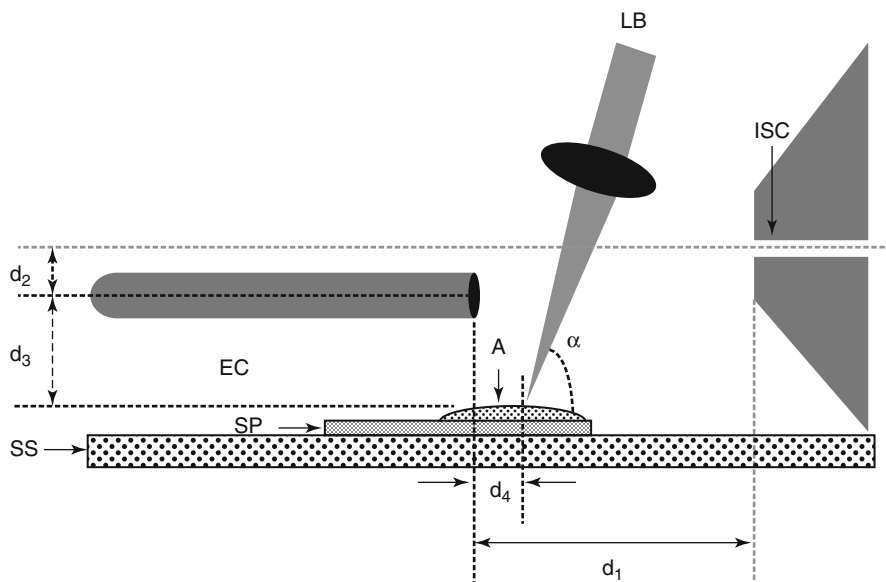


Fig. 13.16 ELDI setup. A analyte, SP: stainless steel sample support plate, SS mobile sample stage, EC electrospray capillary, LB UV laser beam, ISC ion sampling capillary of the API interface. The distances d_1 through d_4 are all in the order of millimeters (Reproduced from Ref. [55] with permission. © John Wiley & Sons, Ltd., 2005)

laser is adjusted to irradiate the sample sideward at an angle of about 45° while spraying (Fig. 13.16).

Effect of the laser in ELDI The combined use of ESI and LDI in ELDI is demonstrated for a sample of neat bovine cytochrome c on a stainless steel target (Fig. 13.17). The first spectrum (A), basically a blank spectrum, was obtained under pure LDI conditions. Spectrum B was measured with ESI on, but no laser irradiation. Finally, spectrum C was generated with both ESI and LDI active. It clearly shows the charge state distribution of the protein as typical for ESI spectra. The advantage of ELDI is that samples can be presented to the inlet nozzle directly from the outside as compared to ESI or MALDI that require additional sample preparation [55].

ELDI has also been applied to the analysis of peptides and proteins [56] even from biological media [57], to detect chemicals on different surfaces [58], and of course, for compound identification on TLC plates [59]. It has been found that addition of a matrix is beneficial for the laser desorption part of the method. This gave rise to *matrix-assisted laser desorption electrospray ionization* (MALDESI) [60].

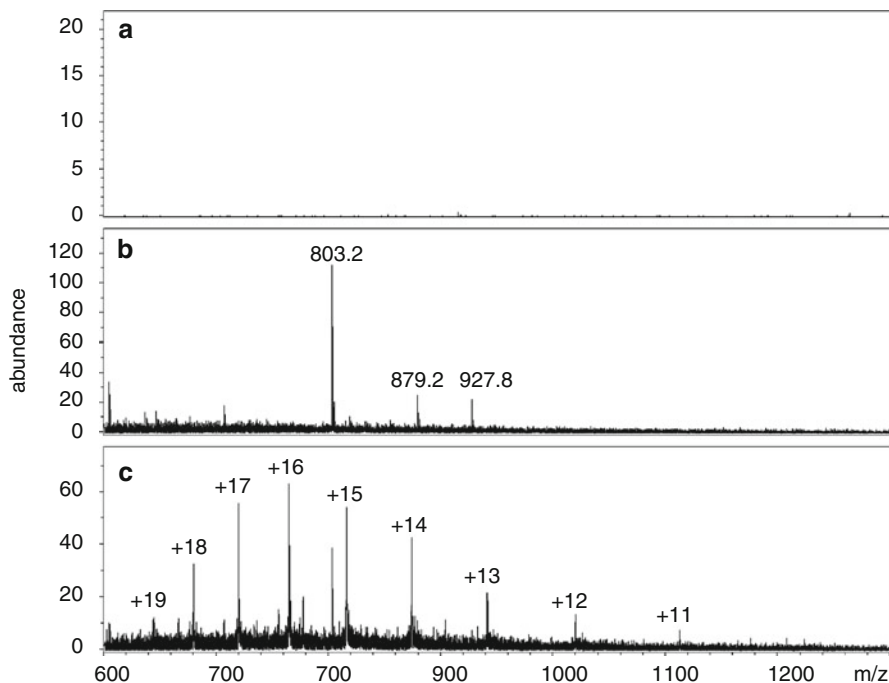


Fig. 13.17 Effect of the combined use of ESI and LDI in ELDI for a sample of neat bovine cytochrome *c*. *Spectrum* (a) was obtained under laser desorption only; (b) under ESI only; and (c) with both ESI and LDI active (Reproduced from Ref. [55] with permission. © John Wiley & Sons, Ltd., 2005)

13.5.4 Laser Ablation Electrospray Ionization

As just described, ELDI and MALDESI require pretreated samples, making them unfavorable for the (*in vivo*) analysis of water-rich biological samples that would preferentially be examined under ambient conditions. By replacing the UV laser with an IR laser (Er:YAG laser of 2.94 μm wavelength), the energy may directly be coupled into the OH vibrational modes of water-rich samples such as tissues. This experimental approach has been termed *laser ablation electrospray ionization* (LAESI) [61–63]. In contrast to AP-IR-MALDI, in LAESI the infrared laser only ablates neutrals from the sample, a noteworthy amount of them even in particulate state, which could be ascertained by flash shadowgraphy [61]. The laser impinging on the sample surface at 90° creates a plume that intercepts an electrospray operating in the cone-jet mode parallel to and at about 25 mm distance from the sample surface. The electrospray post-ionizes the neutrals and the particulate matter in that plume and transports the incipient analyte ions along the spray axis into the sampling orifice of an orthogonal acceleration time-of-flight (oa-TOF) mass spectrometer [61]. Apart from the IR laser, the experimental setup is sufficiently similar to ELDI to omit a schematic here.

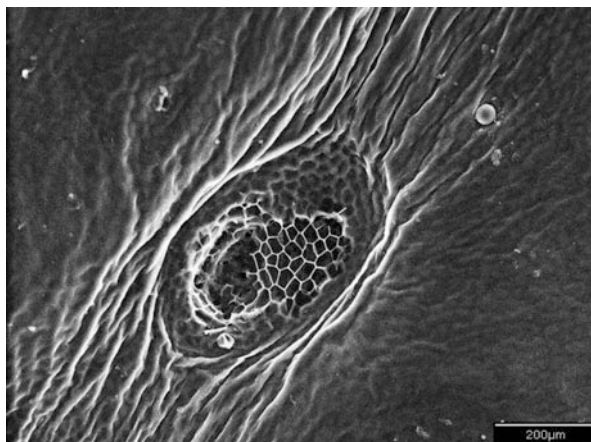


Fig. 13.18 Scanning electron microscope image of the ablation crater produced by a single laser pulse on the adaxial leaf surface of a Zebra plant (*Aphelandra squarrosa*). Scale bar corresponds to 200 μm . Multiple laser pulses penetrated deeper. The wrinkles on the cuticle were caused by the collapse of the underlying cells due to rapid water loss in the vacuum environment during SEM imaging (Adapted from Ref. [62] with permission. © The American Chemical Society, 2008)

In order to minimize the interference of external electromagnetic fields and air currents the LAESI system is shielded by a Faraday cage and a plastic enclosure, respectively. The enclosure also provides protection from potential health hazards of the fine particulates generated in the laser ablation process.

Tissue analysis by LAESI For LAESI, tissue samples are mounted on microscope slides, positioned 10–30 mm below the spray axis and 3–5 mm ahead of the emitter tip, and ablated using an Er:YAG laser with a pulse length of <100 ns and 5 Hz repetition rate. The scanning electron microscope image of the ablation crater produced by a single laser pulse on the adaxial leaf surface of a Zebra plant (*Aphelandra squarrosa*) is shown below (Fig. 13.18). The waxy cuticle and some of the upper epidermal and palisade cells were removed from a slightly elliptical area with axes of 300 and 280 μm indicating effective ablation of tissue [62]. This way, LAESI offers lateral mapping of metabolite distributions and their variations with depth on plant leaves. However, at present, LAESI cannot compete with vacuum imaging methods such as SIMS or MALDI [61].

13.6 Rapid Evaporative Ionization Mass Spectrometry

We have already discussed the impressive capabilities of biotyping and tissuotyping in the context of MALDI-MS (Sects. 11.5 and 11.7). However, MALDI bio- and tissuotyping are restricted to *in vitro* samples. What, if such valuable mass spectral

information was also available in real time by use of some ambient MS technique? In fact, *rapid evaporative ionization mass spectrometry* (REIMS) permits the immediate identification of bacteria, fungi, and other microorganisms [64], and moreover, REIMS opens the road to *in situ* and *in vivo* tissue analyses [65].

13.6.1 Setup of Rapid Evaporative Ionization Mass Spectrometry

REIMS was developed for mass spectral tissue analysis in real time during surgical interventions employing electrosurgical dissection of the tissues. Electrosurgery employs high-frequency electric current for tissue ablation, cutting, and coagulation [65]. The current is directly applied onto the tissues, where it cuts due to thermal damage. Cutting is accompanied by the formation of surgical smoke containing both positively and negatively charged droplets. These charged droplets provide the basis for ion formation analogous to ESI (Sect. 12.4). The charged aerosol can be supplied to the mass spectrometer by modifying the cutting electrode to incorporate a 0.125-inch inner diameter stainless steel tubing that is connected to the API interface via an up to 2-m-long PTFE tubing. The transport of the aerosol from the electrosurgical blade to the interface is driven by a Venturi gas jet pump that aspirates the aerosol from the surgical site. The exhaust of the PTFE line is then positioned near the inlet orifice. An orthogonal orientation of the exhaust line relative to the ion transfer capillary minimizes contamination of the atmospheric pressure interface. An analogous setup with electric current applied to a bipolar forceps can be employed for bacteria and tissue samples alike (Fig. 13.19) [65, 66].

13.6.2 REIMS Spectra

Depending on the chosen polarity, REIMS of biological tissues or microbial samples either generates protonated or deprotonated molecules, mostly of lipids and their thermal degradation products, e.g., fatty acids (Fig. 13.20). When REIMS is applied to the analysis of aqueous solutions of amino acids, pharmaceuticals, or peptides it also yields protonated or deprotonated analyte molecules accompanied by alkali metal and/or ammonium ion adducts. Analogous to ESI, radical ions are not observed in REIMS spectra [65, 66].

13.6.3 REIMS in the Operating Room

As mentioned above, REIMS is intended for online monitoring of tissue being cut during surgery. The quick and unequivocal identification of carcinomatous tissue among healthy parts of an organ is of utmost importance for the surgeon. Traditional histopathological analysis means time-consuming microscopic examination of tissue sections. REIMS is sensitive enough to even allow for combination with

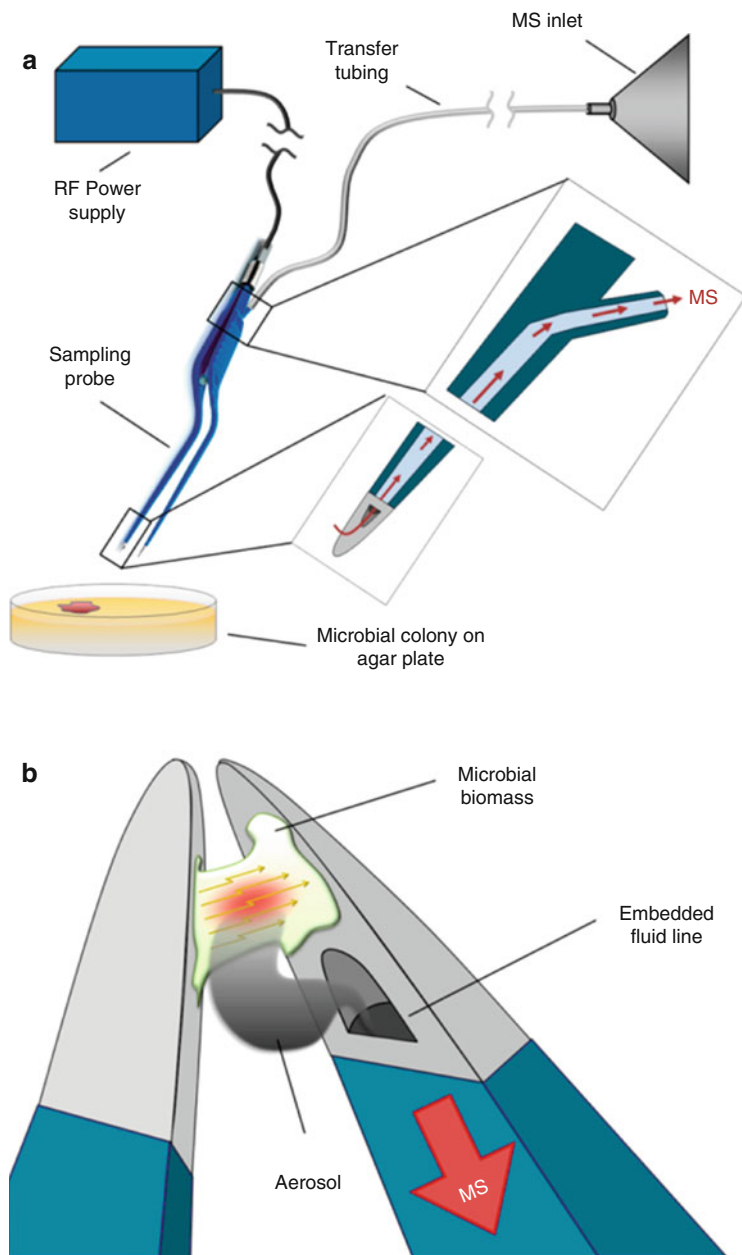


Fig. 13.19 (a) Setup used for analysis of bacteria by REIMS. (b) Scheme of analysis. Microbial biomass is held between the two electrodes of the irrigated bipolar forceps, electrical current is applied, sample is evaporated thermally, and the produced aerosol is aspirated into the opening of the embedded fluid line (Reproduced from Ref. [67] with permission. © American Chemical Society, 2014)

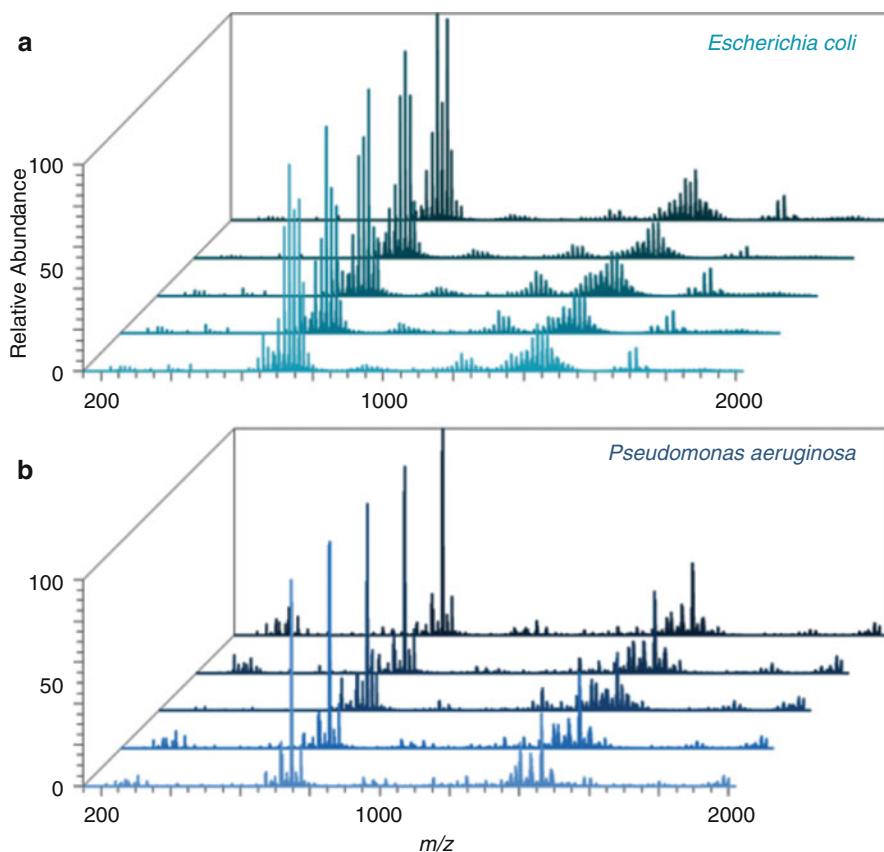


Fig. 13.20 REIMS spectra of different bacteria. (a) *Escherichia coli* and (b) *Pseudomonas aeruginosa*, each grown on five different solid growth media (Adapted from Ref. [67] with permission. © American Chemical Society, 2014)

endoscopic electrosurgery tools and it permits for mass spectra to be obtained in real time (Fig. 13.21) [66].

In the context of clinical applications, REIMS can also serve for high-throughput identification of clinically important bacteria and fungi [64] as well as for the analysis of bulk tissue and bacterial colonies on growth media [68]. Further, REIMS can be used in the detection of food fraud, e.g., to distinguish meat products from cattle, horse, or venison [69].

Whatever the origin of samples may be, their differentiation normally relies on using statistical tools such as principal component analysis (PCA), because the differences between spectra of healthy and infected tissue, for example, are often not immediately visible from the spectra.

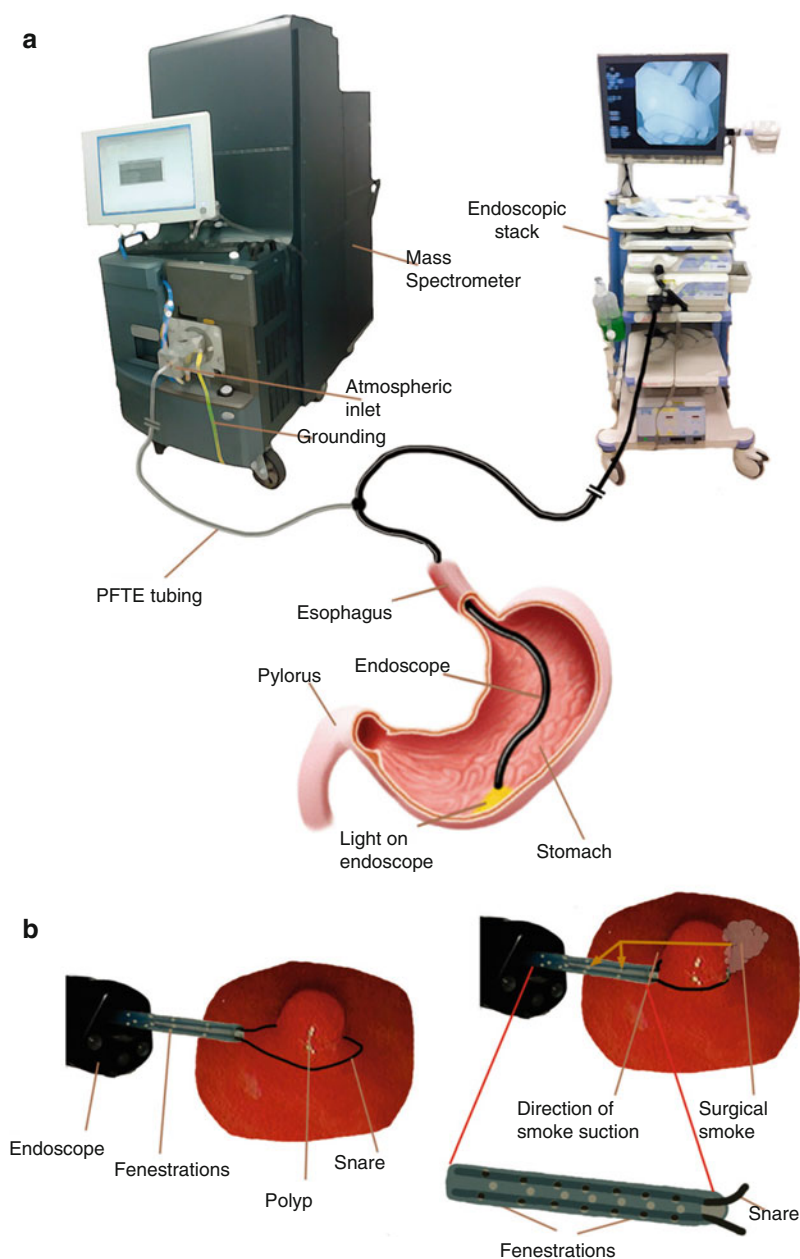


Fig. 13.21 Endoscopy experimental setup. (a) The polypectomy snare was equipped with an additional T-piece in order to establish direct connection between the electrode tip and the mass spectrometer for the transfer of electrosurgical aerosol. (b) Resection of GI polyps by using a commercial snare. The polyp is captured with the snare loop, which is tightly fastened around its base. Electrosurgical dissection is performed and the generated aerosol is aspirated through the fenestrations created on the plastic sheath of the snare (Reproduced from Ref. [66] with permission. © Wiley, 2015)

Recognizing gastric carcinoma Gastric mucosa, gastric submucosa, and adenocarcinoma tissue were analyzed by REIMS using a modified Waters Xevo G2-S Q-ToF mass spectrometer. Both, cancerous and healthy mucosal tissues were found to feature mainly phospholipids in the m/z 600–900 region, whereas submucosa mainly showed triglyceride and phosphatidylinositol species in the m/z 850–1000 region. In this case, even a visual comparison of the abundances of selected peaks shows significant differences between cancerous and healthy tissues in the range m/z 600–1000 (Fig. 13.22). Nonetheless, the recognition is notably simplified by translation of the spectral data in statistically evaluated plots (Kruskal–Wallis ANOVA test).

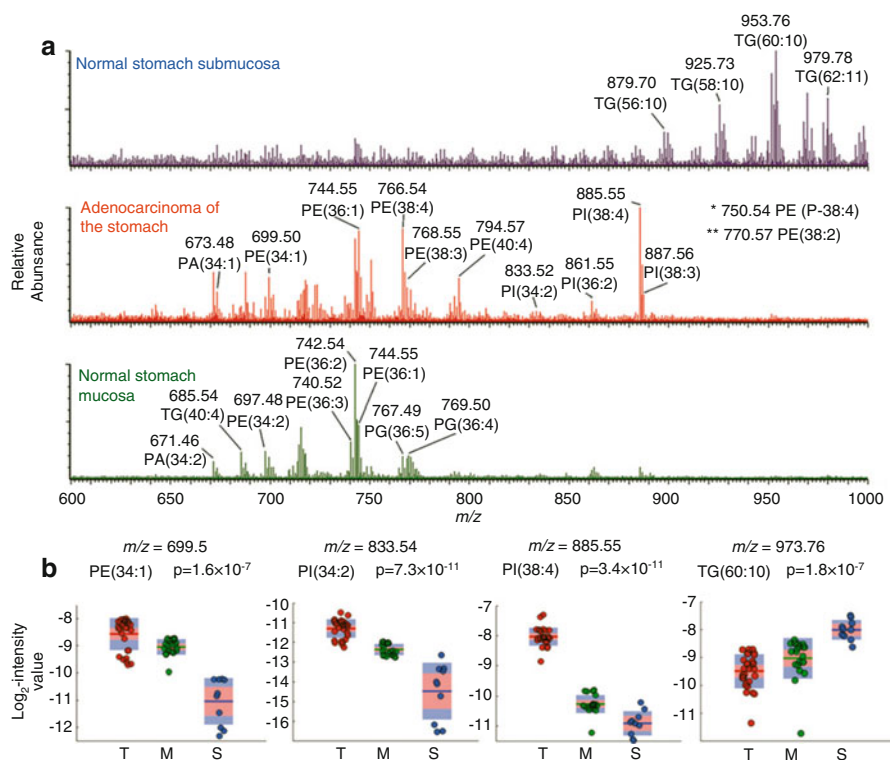


Fig. 13.22 (a) Mass spectra from gastric mucosa, gastric submucosa, and adenocarcinoma tissue recorded *ex vivo*. (b) Comparison of the abundance of selected peaks showing significant differences between cancerous and healthy tissues in the range m/z 600–1000 using Kruskal–Wallis ANOVA, $p < 0.005$. T tumor, M mucosa, S submucosa (Reproduced from Ref. [66] with permission. © Wiley, 2015)

13.7 Atmospheric Pressure Solids Analysis Probe

The *atmospheric pressure solids analysis probe* (ASAP) [70, 71] addresses a more classical field of organic mass spectrometry: the analysis of small organic molecules. With the successive replacement of classical EI and CI instrumentation – mostly magnetic sector instruments equipped with direct insertion probes – by APCI (Sect. 7.8), ESI (Chap. 12) or MALDI (Chap. 11) instruments, the tools to deal with samples that would previously have been run by EI-MS or CI-MS have been phased out in many MS laboratories. Based on a modification to an APCI source, ASAP offers an alternative to EI (Chap. 5) or CI (Chap. 7). Thus, ASAP can fill this gap in the MS toolbox at least to some extent [70].

13.7.1 Setup of the Atmospheric Pressure Solids Analysis Probe

In ASAP, by simply inserting a melting point tube into a stream of hot nitrogen gas, the solid is evaporated from the tube's surface and then ionized at atmospheric pressure by the corona discharge of an APCI source. The hot gas stream (350–500 °C) may either be provided by the APCI sprayer or by an ESI sprayer, provided the latter features a heated desolvation gas supply. In contrast to DESI or DAPCI, no solvent flow is employed in ASAP. Thus, the only modification of a commercial APCI source is to machine a small port into the housing around the spray region for insertion of the glass tube or to seal the hole by a plug when switching back to standard APCI or ESI operation (Fig. 13.23). ASAP devices are commercially available [72] but can also be custom-built with comparative ease [70, 73].

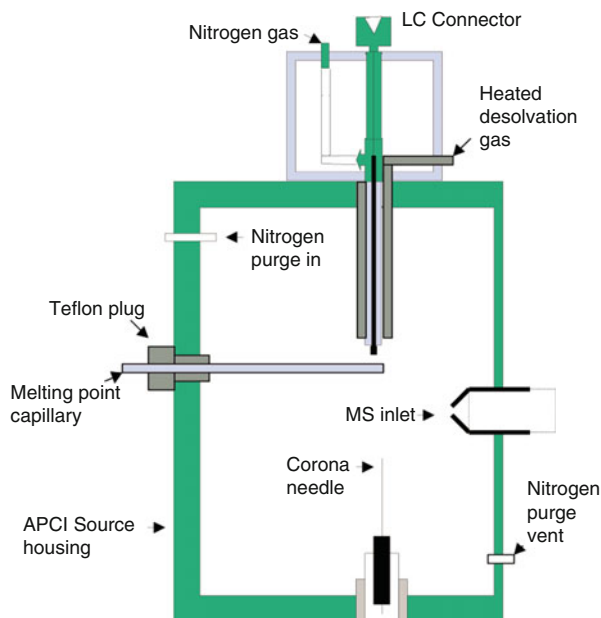
Not exactly ambient MS

ASAP does not strictly meet the criteria of ambient MS, in particular, if we define ambient MS by its ability to perform surface analysis of an object exposed to some ionizing fluid in the open atmosphere. ASAP requires the application of sample to a probe and it is performed inside a closed housing. Apart from the welcome association with the acronym, ASAP would have better been termed *probe-APCI*. Nonetheless, ASAP also bears some characteristics of ADI-MS.

13.7.2 Atmospheric Pressure Solids Analysis Probe in Practice

As in APCI, the analytes addressed by ASAP may range from low to high polarity and can have molecular masses in the 100–1500 u range. Representative applications of ASAP include screening for plasticizers in food packaging [74], the analysis of low-molecular-weight synthetic polymers [72], the high-throughput identification of anabolic steroid esters in the screening of drugs [75], or the

Fig. 13.23 Cross section of an atmospheric pressure solids analysis probe (ASAP) based on the standard APCI source of a Waters Q-TOF instrument (Reproduced from Ref. [70] with permission. © American Chemical Society, 2005)

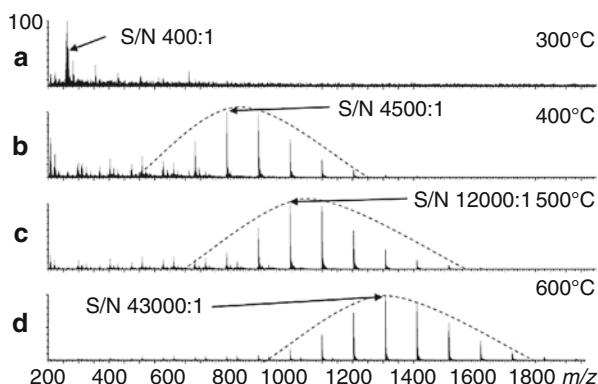


analysis of nucleosides [73]. ASAP can also be used in conjunction with ion mobility-mass spectrometry as demonstrated for the detection and identification of impurities in 2-naphthalenamines [76].

One should be aware that application of sample onto the outside of a glass capillary, in particular, when provided as powder, inherently bears the risk of ion source contamination, e.g., during the process of inserting the capillary. Also, there is a tendency that dipping applies too large amounts of sample that may lead to cross contamination in subsequent runs. Therefore, care needs to be exercised to avoid these problems.

Oligomer analysis by ASAP Polystyrene of an average molecular weight of $M_n = 1700$ u (PS1700) was applied to the exterior of a glass capillary by dipping it into the PS powder. Positive-ion spectra in the m/z 50–2000 range were recorded using a Waters ASAP source mounted onto a Xevo QToF instrument. The majority of ion source parameters were set as typically the case in APCI operation (corona needle at 3.0 kV, corona discharge at $2.5 \mu\text{A}$, nitrogen gas at 600 l min^{-1}). The temperature of the nitrogen was stepwise increased from 300 to 600°C . The ASAP spectra showed a clear correlation between this temperature, the m/z range covered with PS signals, and the signal-to-noise ratio (S/N) achieved (Fig. 13.24) [72]. A minimum of 400°C was required to form some PS ions at all, that showed up as molecular ions. Obviously, the low-polarity PS was ionized by charge transfer to form $M^{+\bullet}$ ions. While the range covered was able to be expanded up to higher m/z , even the

Fig. 13.24 The effect of desolvation gas temperature upon ASAP of polystyrene at (a) 300 °C, (b) 400 °C, (c) 500 °C, and (d) 600 °C (Reproduced from Ref. [72] with permission. © The Royal Society of Chemistry, 2012)



spectrum at 600 °C did not fully meet the M_n for this sample as derived from gel permeation chromatography (GPC).

13.8 Direct Analysis in Real Time

Direct analysis in real time (DART) [3], similar to ASAP in the preceding section, employs a solvent-free heated gas stream. In contrast to the aforementioned techniques, the DART gas initially carries excited noble gas atoms that have been formed in a plasma discharge. Reagent ions are then formed immediately upon interaction of these electronically excited atoms with the atmosphere. Thus, DART is related to atmospheric pressure chemical ionization (APCI) [5] and also bears some similarity to DAPCI or DAPPI.

Like DESI, DART sources are commercially available. As a powerful and highly versatile technique of ambient MS, DART has seen a vast number of applications [5, 6, 8, 9, 77–87].

13.8.1 DART Ion Source

In a DART source, a gas flow, typically helium or rarely nitrogen, is guided through a tube divided into three segments. In the first section, a corona discharge between a needle electrode and a first perforated disk electrode produces ions, electrons, and excited atoms (Fig. 13.25). The gas discharges in DART can be visibly distinguished as nitrogen emits a clear blue glare while the helium discharge shines in pale pink (Fig. 13.26).

The cold plasma passes through a further chamber where a second perforated electrode can remove cations from the gas stream that is subsequently heated and passed through a final grid electrode removing oppositely charged species. The ionizing neutral gas may either be directed towards the sampling orifice of an API

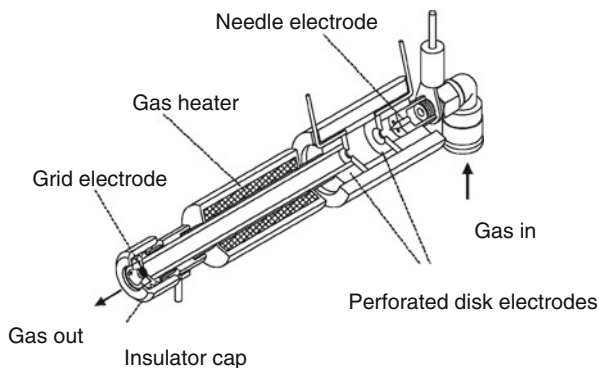


Fig. 13.25 Cutaway view of the DART source. The emanating gas effects ionization of sample independent of its state of aggregation (Reproduced from Ref. [3] with permission. © The American Chemical Society, 2005)

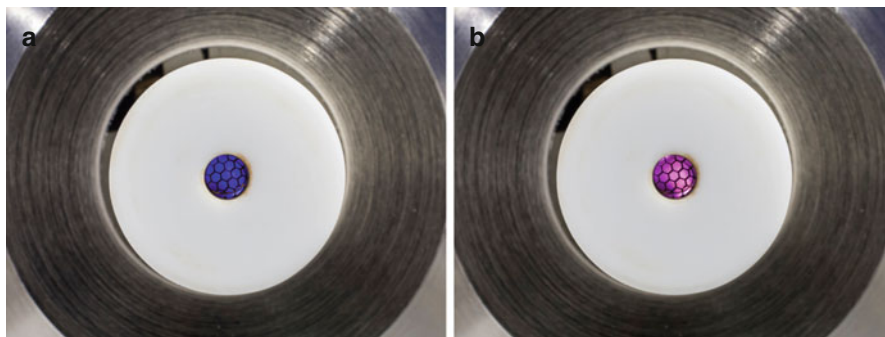


Fig. 13.26 DART discharges as seen when looking into the source. (a) Blue shining discharge in nitrogen, (b) pale pink discharge in helium. The hexagonal pattern is caused by the exit grid electrode

interface, or analogous to DESI, may hit the sample surface at an angle suitable for its reflection into the entrance of the mass spectrometer [3].

Typical operating conditions for DART use a positive discharge needle potential of 1–5 kV while the counter electrode (first perforated disk electrode) is grounded. The potentials of the second perforated electrode and the exit grid electrode are set to positive potentials for positive-ion DART and to negative potentials in the order of a hundred volts for negative-ion mode. The insulator cap protects sample and operator from any high voltage. The gas flow is adjusted to 1–3 l min⁻¹ and the gas temperature may vary in the range of 50–500 °C. The DART source is adjustable over a range of angles and distances. Typically, a gap of 5–25 mm is established to insert the sample.

Type of the discharge

The DART discharge belongs to the corona-to-glow (C-G) discharge type that operates with discharge currents in the order of 2 mA at a temperature of 50–60 °C [88]. Recently, efforts have been made to provide a more efficient source for metastable atoms. A direct current *atmospheric pressure glow discharge* (APGD) sustained in helium and used in the *flowing afterglow* (FA) mode seems promising [88–90].

13.8.2 Positive Ion Formation in DART

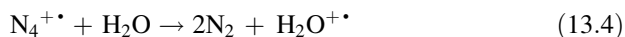
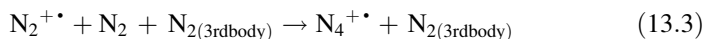
The electrical discharge in helium produces a stream of gas containing electronically excited helium atoms (metastable atoms), ions, and electrons:



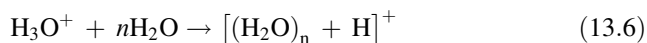
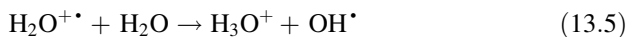
The plasma gas is then heated and fully depleted of ions and electrons by passing it through electrically charged grids. When the stream exits to the open atmosphere, it may effect ionization of gases, and by direct contact also liquids and solids. The majority of the metastable helium atoms, He^* , induces *Penning ionization* (Sect. 2.1.3) of nitrogen [3, 89]:



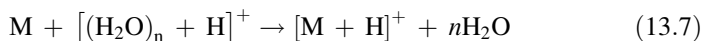
Apart from initiation by a discharge that delivers metastable helium atoms, He^* , carrying 19.8 eV of energy, the pathway of reagent ion formation in DART basically follows the same route as in APCI (Sect. 7.8). Ion–molecule reactions are fast at atmospheric pressure due to high collision rates ($> 10^9 \text{ s}^{-1}$). Seemingly bimolecular reactions often are termolecular in reality, because a neutral collision partner like N_2 in Eq. 13.3 is required for immediate removal of excess energy [91–94]. Thus, the next steps lead to water molecular ions:



Then, the $\text{H}_2\text{O}^{+\bullet}$ ions quickly form cluster ions:



Finally, the $[(\text{H}_2\text{O})_n + \text{H}]^+$ ions act as reagent ions for analyte ion formation by protonation [93]:

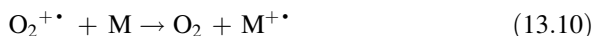
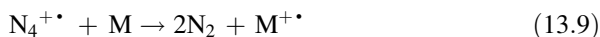


Ammonium ion adducts are also observed in DART of medium polar compounds. $[\text{M} + \text{NH}_4]^+$ ions occur, for example, with oxygen-rich molecules, in particular in the absence of basic functional groups, e.g., polyethylene glycols, ketones, di- or triacylglycerols, and polysiloxanes:



Ammonium ions may be delivered along with the sample, can be formed from trace amounts of ammonia in the atmosphere, or can intentionally be supplied simply by placing a vial with aqueous ammonia close to the reaction zone.

In addition to even-electron ions, DART can also yield odd-electron ions by charge transfer, i.e., DART can deliver molecular ions [95, 96]. Analyte molecular ions, $\text{M}^{+\bullet}$, can either be generated by Penning ionization with He^* or more importantly by charge transfer. In the open atmosphere, the reagent ions are $\text{N}_4^{+\bullet}$, $\text{O}_2^{+\bullet}$, and NO^+ :



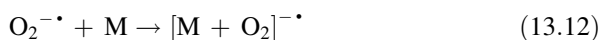
The ratio of $\text{M}^{+\bullet}$ versus $[\text{M} + \text{H}]^+$ ion formation is mainly determined by analyte properties such as ionization energy, IE , and proton affinity, PA [97]. Low IE is going to favor $\text{M}^{+\bullet}$ ions while high PA promotes $[\text{M} + \text{H}]^+$ ion formation. Depending on the analyte, both ionic species can occur simultaneously causing the superimposition of $\text{M}^{+\bullet}$ and $[\text{M} + \text{H}]^+$ ion signals. Distorted isotopic patterns present a drawback for spectrum interpretation.

Helium may be replaced by argon as the DART gas in order to provide more selective or softer ionization, respectively [98, 99]. Unfortunately, argon has energetically lower metastable states of 11.55 eV ($^3\text{P}_2$) and 11.72 eV ($^3\text{P}_0$) and cannot ionize water ($IE = 12.65$ eV), causing argon-DART to have much lower sensitivity. It can be improved by a solvent make-up flow into the reaction zone, e.g., $IE_{\text{MeOH}} = 10.85$ eV. The ionization mechanism then switches from a $\text{H}_2\text{O}^{+\bullet}$ -based pathway to a solvent ion-based process (replace H_2O by MeOH in Eqs. 13.4, 13.5, 13.6 and 13.7) [98, 99].

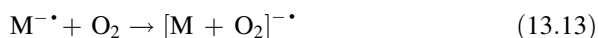
Whatever the actual process of ion formation, the high collision rates at atmospheric pressure effect immediate thermalization. As generally the case in ADI-MS, fragmentation is not really relevant in DART-MS.

13.8.3 Negative Ion Formation in DART

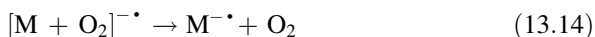
In negative ion mode, thermal electrons created by the reaction in Eq. 13.2 are presumed to generate mostly $O_2^{\cdot-}$ ions from air that serve as reagent ions. Of course, direct electron capture by the analyte as well as dissociative electron capture, deprotonation, or anion attachment are also feasible [92]. These $O_2^{\cdot-}$ ions form adducts by association with the analyte M:



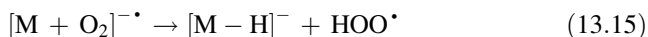
Alternatively, negative molecular ions directly formed by electron capture can attach to molecular oxygen, thereby yielding the same product:



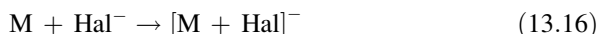
$[M+O_2]^{\cdot-}$ may either be detected as such or may dissociate to yield radical anions:



The loss of a hydroperoxyl radical may lead to $[M-H]^-$ ions, i.e., proton abstraction, if the gas phase acidity of $[M-H]^-$ exceeds that of HOO^{\cdot} :



Apart from $O_2^{\cdot-}$, the atmospheric components lead to $NO_2^{\cdot-}$, $CO_3^{\cdot-}$ [100], and depending on traces of solvents also CN^- , Cl^- , OH^- , and other ions. Halogenide adduct ions can be observed when the analyte and/or a solvent are halogenated:



Finally, adduct ion formation with less abundant anions such as CO_3^- , NO_2^- , or OH^- can occur.

13.8.4 ADI Methods Related to DART

There are numerous ion sources that similarly rely on Penning ionization. Some of them preceded DART by many years while the development of others may have been inspired by DART. Most of these techniques never became commercially available, and thus, sometimes are unique to a single research group. DART is the by far best established technique in the field.

Penning ionization represents only one facet of DART as it is the primary source of ionization for DART. Rather than direct Penning ionization of the analyte, in most cases reagent ions derived from atmospheric components are responsible for analyte ion generation. DART can therefore be categorized as belonging to a family

Table 13.2 Methods of ambient mass spectrometry closely related to DART

Full term	Acronym	References
Liquid surface Penning ionization	LPI	[102, 103]
Atmospheric sampling glow discharge ionization	ASGDI	[104]
Atmospheric pressure Penning ionization	APPeI	[105–107]
Plasma-assisted desorption/ionization	PADI	[108]
Dielectric barrier discharge ionization	DBDI	[109, 110]
Double cylindrical barrier discharge ionization	DC-DBDI	[111]
Atmospheric pressure glow discharge ionization	APGD	[112]
Helium atmospheric pressure glow discharge ionization	HAPGDI	[112]
Flowing afterglow atmospheric pressure glow discharge	FA-APGD	[90]
Low-temperature plasma probe	LTP	[101]
Atmospheric pressure solids analysis probe	ASAP	[70, 71, 113]
Surface-activated chemical ionization	SACI	[114, 115]
Desorption atmospheric pressure chemical ionization	DAPCI	[14, 21, 31, 101]
Desorption atmospheric pressure photoionization	DAPPI	[16]
Atmospheric pressure thermal desorption ionization	APTDI	[116]

of APCI-related ionization techniques [4]. DART and other techniques of this group have in common that they use a stream of heated gas containing ionizing species that are created in some sort of an atmospheric pressure plasma [101].

For completeness, these related techniques are compiled in Table 13.2. The multiple relationships between most of the numerous techniques mentioned here, have been visualized in a “flowergram” (Fig. 13.27) [5].

13.8.5 DART Configurations

In contrast to the gases normally contained in air, helium presents a true challenge for all types of vacuum pumps. The JEOL AccuTOF instrument that DART was originally developed for happens to possess some zig-zag ion path in the ion source optics that guides ions to the orthogonal TOF analyzer while it deflects neutrals. Thus, the use of helium was easily accepted by this instrument [3]. However, helium flow into the API interface of mass spectrometers other than the JEOL AccuTOF would cause poor if not unacceptable vacuum conditions when the DART source is in operation. To solve this problem, the so-called Vapor Interface is mounted in between the DART source and the entrance of the API interface where it serves as an additional pumping stage. A small membrane pump suffices to remove most of the helium. Furthermore, the aspirating ceramics tube improves the ion transfer from the ionization zone into the mass spectrometer (Fig. 13.28).

Initially, the DART source was configured on-axis with the sampling orifice of the API interface and objects to be analyzed were positioned tangentially to present the surface to the helium flow. Notable improvements for the analysis of single compounds and simple mixtures were made by the introduction of transmission mode DART

Fig. 13.27 Relationship of DART to other methods of ambient MS that basically rely on APCI-like mechanisms of ion formation. A “flowergram” illustrates the methods (*red*) where chemical ionization processes (*yellow*) are used for analyte ion formation. Reagent ion generation (*green*) is initiated by either plasma, corona discharge, ion evaporation, or photoionization (Reproduced from Ref. [5] by kind permission. © Elsevier, 2008)

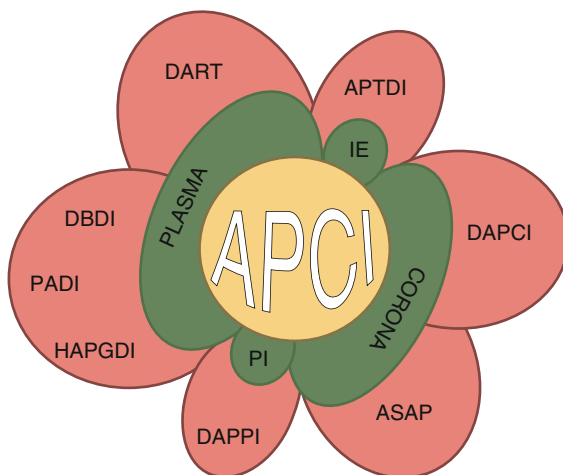
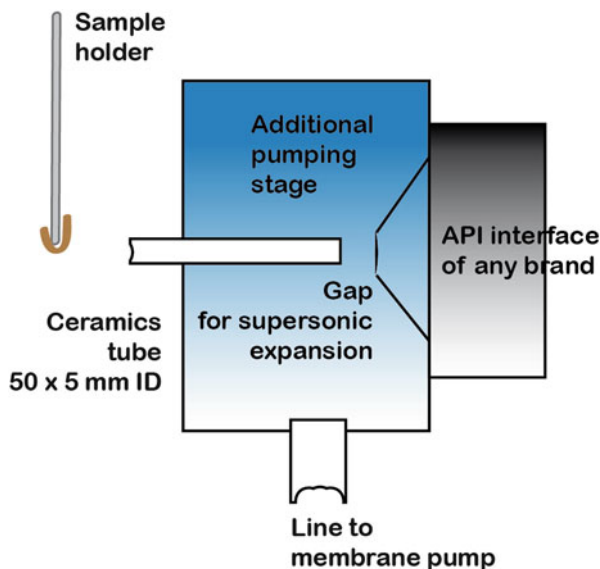


Fig. 13.28 Schematic of the Vapor Interface used to adapt the DART source to API interfaces of different instrument manufacturers. The additional pumping stage prevents compromised instrument vacuum and improves the transfer of sample ions by acting as a jet separator (Reprinted from Ref. [8] with permission. © Springer, 2013)



[117]. For transmission mode, the sample is deposited on a fine wire mesh that is then immersed into the gas stream; the mesh provides both a large surface and good transmission for the ion-carrying gas. For the DART analysis of objects, an angled configuration as used in DESI turned out to be more efficient [118]. As a consequence, DART sources can be configured in various ways to optimally meet the requirements of a variety of samples (Fig. 13.29) [8]. For routine analyses in synthetic chemistry, the Open Source, a special device for use with disposable sample cards, provides the most facile way of transmission mode DART-MS while the 45° geometry is best suited for surface mode DART (Fig. 13.30).

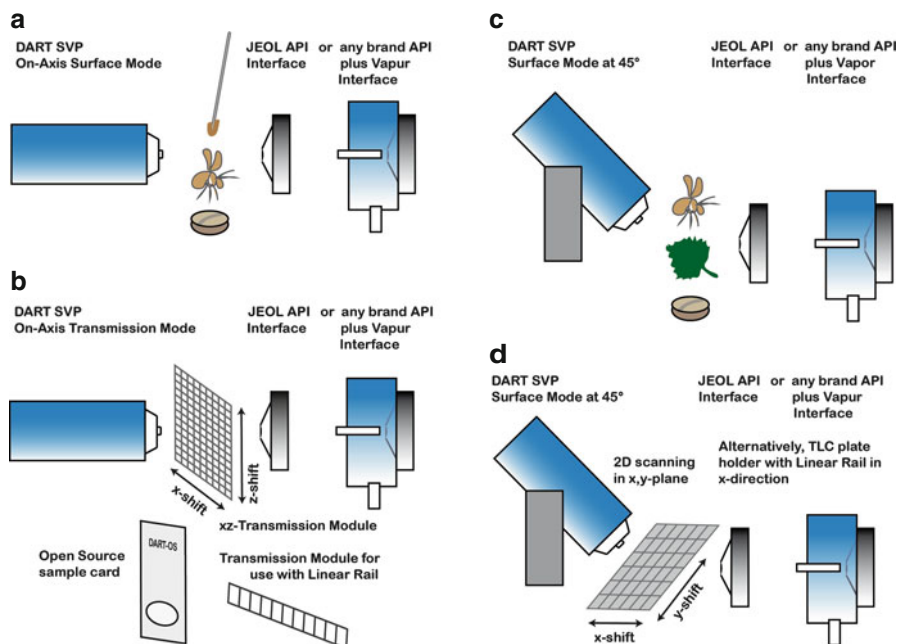


Fig. 13.29 DART configurations. (a) First design with axial orientation of source and orifice of the API interface, (b) axial orientation for transmission mode when presenting samples on a mesh, (c) surface mode with source at an angle for analyzing small objects, and (d) surface mode at an angle for automated analysis of an array of samples (Adapted from Ref. [8] with permission. © Springer, 2013)

13.8.6 Analytical Applications of DART

From the very beginning, DART has been applied to the most diverse kinds of cases [5, 6, 8, 9, 77–87]. This includes the typical safety-related and forensic usages of ambient MS like detection of explosives, warfare agents, or pharmaceuticals and drugs of abuse from cloth, banknotes, etc. [3, 92, 119], or the examination of ballpoint-pen inks on paper, e.g., signatures in cases of check fraud [120]. In the life sciences, DART serves for the rapid analysis of fatty acid methyl esters (FAMES) from whole cells [121], for clinical studies of compounds from plasma and urine [122, 123]. DART is sensitive enough to analyze self-assembled thiol and dithioether monolayers on gold surfaces [124]. Some representative applications are depicted below to give an idea of the manifold uses of DART-MS.

Volatiles from garlic Positive-ion and negative-ion DART-MS was used for the identification of reactive sulfur-containing compounds formed from cutting different species of the genus *Allium* (garlic, onion, elephant garlic, leek, Chinese chives, and others) [125, 126]. Garlic cloves were held into the open gap between the DART source and the orifice of the API interface of a JEOL AccuTOF instrument

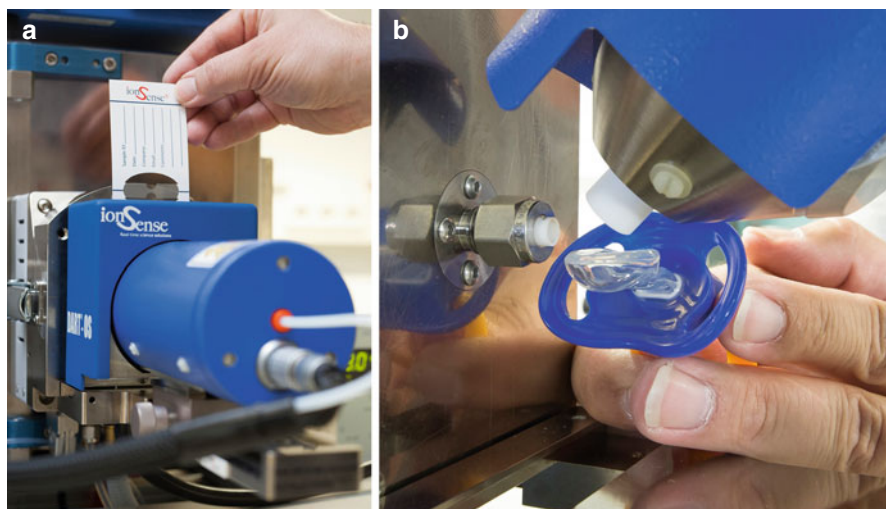


Fig. 13.30 DART configurations in use. (a) Open Source for transmission mode DART with disposable sample cards (corresponds to setup b in Fig. 13.29), (b) alignment at an angle of 45° for the analysis of objects placed in the gap (corresponds to setup c in Fig. 13.29). Both photos show the DART source attached to a Bruker instrument by means of the Vapur Interface



Fig. 13.31 Commercial DART source of the first generation on a JEOL AccuTOF instrument. Here it is used for the analysis of volatiles from a garlic clove [125, 126]. The sample is simply held into the open gap between the metastable atom source (*lower right part*) and the orifice of the API interface (*upper left*). Photograph by courtesy of JEOL USA

(Fig. 13.31 and mode a in Fig. 13.29). From cut garlic, for example, positive-ion DART showed compounds such as allucin, allyl/methyl and dimethyl thiosulfinates, diallyl trisulfane *S*-oxide, allyl alcohol, and propene. Negative-ion DART detected 2-propenesulfenic acid, 2-propenesulfinic acid, SO_2 , and pyruvate. The different *Allium* species exhibited different volatile compounds.

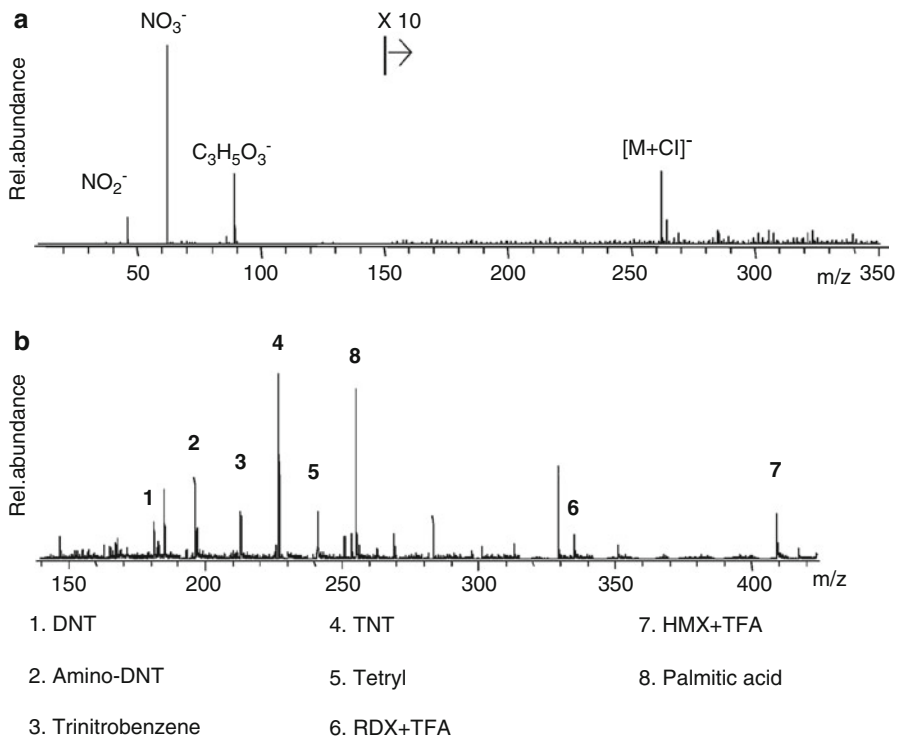


Fig. 13.32 DART spectra of explosives. Spectrum (a) shows nitroglycerin detected on a man's necktie 8 h after exposure to the plume from blasting at a construction site. In (b) a sample of contaminated pond water exhibits $[\text{M}+\text{TFA}]^-$ peaks for various explosives that are present at about 3 ppm (Reproduced from Ref. [3] with permission. © The American Chemical Society, 2005)

Negative-ion DART for explosives Still under the impression of the 2001 terrorist attack on the World Trade Center, ambient MS initially had a strong focus on the detection of explosives. Negative-ion DART is very sensitive for the analysis of explosives exhibiting extremely low but non-zero vapor pressure [92]. Nitroglycerin has been detected on a man's necktie 8 h after exposure to the plume from blasting at a construction site (Fig. 13.32a) and various explosives present at about 3 ppm in a contaminated pond water sample have been detected; placing a small open bottle with 0.1% aqueous trifluoroacetic acid (H-TFA) in proximity to the sampling zone caused them to appear as $[\text{M}+\text{TFA}]^-$ adduct peaks in the DART spectrum (Fig. 13.32b) [3].

Invading a fly's private sphere DART allows for the cuticular hydrocarbon analysis of active fruit flies *Sophophora melanogaster* (*Drosophila melanogaster*). The hydrocarbon profile as measured from the exterior of female flies comprises alkenes and alkadienes in the C_{18} to C_{29} range that are detected as $[\text{M}+\text{H}]^+$ ions. The profile

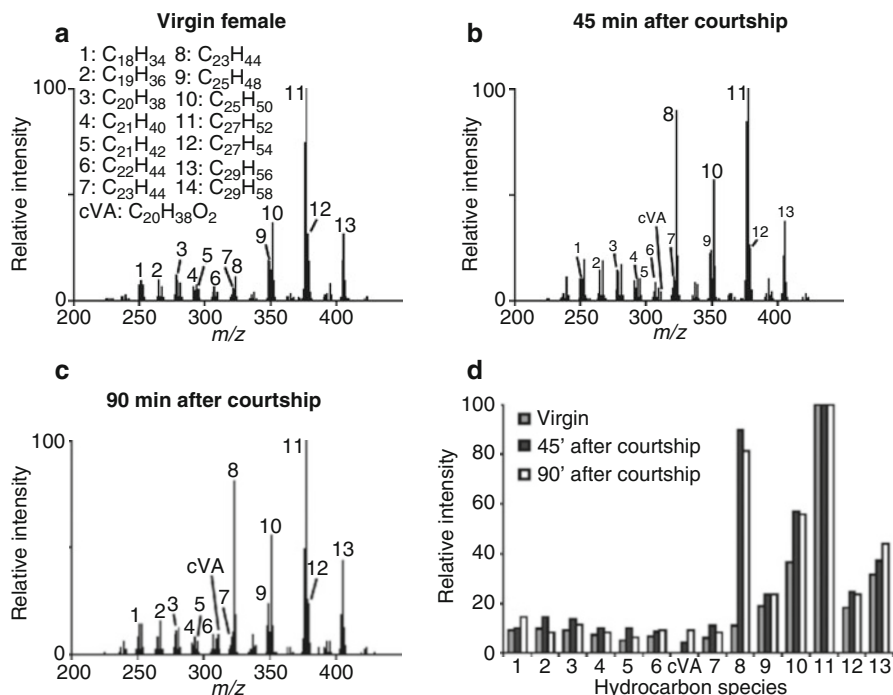


Fig. 13.33 Chemical profile changes in the same individual female fly as observed (a) before, (b) 45 min after, and (c) 90 min after copulation. (d) A histogram shows the changes in hydrocarbon concentrations, in particular, an increase in tricosene (peak 8) and pentacosene (peak 10) (Reproduced from Ref. [127] with permission. © The National Academy of Sciences of the USA, 2008)

has been found to vary depending on whether the flies are observed as virgin females, 45 min or 90 min after courtship (Fig. 13.33). There is also a difference between males and females. The advantage of DART is that the fly can be exposed to the ionizing gas stream without risk of electrical shock to both fly and researcher [127].

Silicones in household utensils and food Positive-ion DART is highly suitable for the analysis of polydimethylsiloxanes (PDMS) [128, 129], commonly known as silicone rubber. Silicone rubber is a common material of articles of daily use such as flexible silicone baking molds, watch bands, dough scrapers, pacifiers, and non-stick coatings of parchment paper, for example [130]. DART not only permits to analyze the household utensils themselves (Sect. 3.6.5) [129] but also to assess their tendency to release low-molecular-weight silicone oligomers into food during baking [129, 131, 132].

For the analysis of the household items, the DART source was mounted at an angle of 45° relative to the axis of the ceramics tube of the Vapor Interface. The entire objects were manually positioned about halfway between the helium exit and

capillary entrance and directly exposed to the ionizing gas (Fig. 13.30b). For all silicone rubber items, the gas was uniformly set to 300 °C. A typical spectrum of baked goods analyzed after use of a silicone rubber baking mold is shown in Fig. 13.34. The m/z 200–1650 range demonstrates the relative intensities of peaks from triacylglycerols (TAGs), i.e., fat from butter, and PDMS (*right*). The series of $[M+NH_4]^+$ ions of low-mass TAGs on average exhibits the characteristic value $\Delta(m/z) = 28.0313$ due to differences by $(CH_2)_2$ units. Series of ions at higher mass with peaks of $\Delta(m/z) = 74.0185$ on average, are caused by PDMS differing by $[(CH_3)_2SiO]$ repeat units. The isotopic patterns also reveal multiple Si atoms [131]. Obviously, there is a substantial release of PDMS into the food [131, 132].

Furthermore, the distribution of peaks across the m/z 200–3000 range permits the use of silicone oil and grease for mass calibration in positive-ion DART-MS [128].

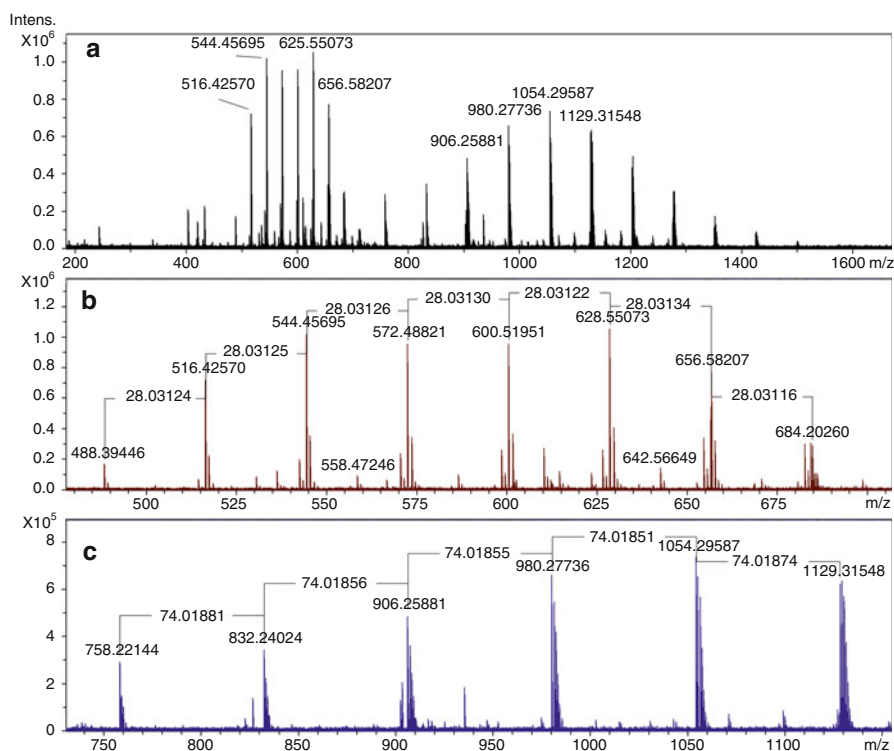


Fig. 13.34 Positive-ion DART spectra of a dough baked in a Kaiser silicone rubber baking mold. (a) Entire spectrum in the m/z 200–1650 range to show the relative intensities of peaks from TAGs (*left*) and PDMS (*right*). (b) Series of $[M+NH_4]^+$ ions of low-mass TAGs exhibiting the characteristic value $\Delta(m/z) = 28.0313$ on average. (c) Series of ions at higher mass with peaks of $\Delta(m/z) = 74.0185$ on average, owing to $[(CH_3)_2SiO]$ repeat units. The isotopic patterns also reveal multiple Si atoms (Reprinted from Ref. [131] with permission. © SAGE, 2015)

13.9 The World of Ambient Mass Spectrometry

Characteristic Feature of Ambient MS

The novel and characteristic feature of *ambient desorption/ionization* (ADI) or *ambient mass spectrometry* is that it allows instantaneous mass spectral analysis without sample preparation or sample pretreatment. Furthermore, the object to be analyzed is handled at atmospheric pressure, i.e., in a freely accessible open space in front of the atmospheric pressure interface.

Ambient MS allows for the examination of untreated samples or entire objects in the open environment while maintaining sample integrity. Ambient MS is elegant in that a sample only needs to be exposed to an ionizing fluid medium under ambient conditions.

A Family of Methods

There is no single method. Instead, the term ambient MS collects a group of techniques that all share the feature of ambient desorption/ionization. ADI-MS employs ion generation based on ESI, APCI, APPI, combinations thereof with laser desorption, and various electrical discharges to create ionizing plasmas as employed in DART.

Methods of Ambient MS

The below short table summarizes some of the more relevant ambient MS methods. They are listed in alphabetical order of their acronyms together with a key reference (Table 13.3). It should be noted, however, that only the truly simple-to-operate yet effective and rugged interfaces will survive over the years. As predicted in the previous edition of this book, DESI and DART were among the ones to persist in the long term.

Applications of Ambient MS

There is a vast range of applications for ambient MS. The major methods DESI and DART are documented in hundreds of publications each and also the numerous other methods were employed in manifold ways, sometimes to solve very specific problems. The development of ADI-MS is being pursued at a high pace.

A Word of Caution

Ambient MS methods tend to be easy to use, and in fact, can be a pleasure to use. While the range of applications is absolutely impressive, one should be aware that any of these methods only reveals what is present *on* the surface. Even there, compounds may be suppressed as others are ionized much more efficiently by the ADI method employed and under the operational conditions actually set. ADI-MS cannot reveal what is *below* the surface. Nonetheless, similar restrictions apply for any other MS method.

Table 13.3 Methods of ambient mass spectrometry

Acronym	Full term	Basic principle and key references
ASAP	Atmospheric pressure solids analysis probe	Evaporation of solids in hot gas stream and ionization by corona discharge [70]
DAPCI	Desorption atmospheric pressure chemical ionization	Sample surface exposed to APCI [21]
DAPPI	Desorption atmospheric pressure photoionization	Sample surface exposed to APPI [16]
DART	Direct analysis in real time	Sample surface exposed to ionizing noble gas stream [3]
DESI	Desorption electrospray ionization	Sample surface exposed to electrospray plume [1, 2]
DeSSI	Desorption sonic spray ionization	Sample surface exposed to sonic spray ionization plume; equal to EASI [10]
ELDI	Electrospray-assisted laser desorption ionization	LDI with post-ionization by ESI plume [55]
EASI	Easy ambient sonic-spray ionization	Sample surface exposed to sonic spray ionization plume; equal to DeSSI [42]
EESI	Extractive electrospray ionization	Sample vapor or mist admixed to electrospray plume [13, 46]
LAESI	Laser ablation electrospray ionization	IR laser ablation with postionization by ESI plume [62]
MALDESI	Matrix-assisted laser desorption electrospray ionization	Uptake of AP-MALDI plume by ESI spray and transport into API interface [60]

References

1. Takats Z, Wiseman JM, Gologan B, Cooks RG (2004) Mass Spectrometry Sampling Under Ambient Conditions with Desorption Electrospray Ionization. *Science* 306:471–473. doi:[10.1126/science.1104404](https://doi.org/10.1126/science.1104404)
2. Takats Z, Wiseman JM, Cooks RG (2005) Ambient Mass Spectrometry Using Desorption Electrospray Ionization (DESI): Instrumentation, Mechanisms and Applications in Forensics, Chemistry, and Biology. *J Mass Spectrom* 40:1261–1275. doi:[10.1002/jms.922](https://doi.org/10.1002/jms.922)
3. Cody RB, Laramee JA, Durst HD (2005) Versatile New Ion Source for the Analysis of Materials in Open Air Under Ambient Conditions. *Anal Chem* 77:2297–2302. doi:[10.1021/ac050989d](https://doi.org/10.1021/ac050989d)
4. Weston DJ (2010) Ambient Ionization Mass Spectrometry: Current Understanding of Mechanistic Theory; Analytical Performance and Application Areas. *Analyst* 135:661–668. doi:[10.1039/b925579f](https://doi.org/10.1039/b925579f)
5. Venter A, Nefliu M, Cooks RG (2008) Ambient Desorption Ionization Mass Spectrometry. *Trends Anal Chem* 27:284–290. doi:[10.1016/j.trac.2008.01.010](https://doi.org/10.1016/j.trac.2008.01.010)
6. Green FM, Salter TL, Stokes P, Gilmore IS, O'Connor G (2010) Ambient Mass Spectrometry: Advances and Applications in Forensics. *Surf Interface Anal* 42:347–357. doi:[10.1002/sia.3131](https://doi.org/10.1002/sia.3131)
7. Weston DJ, Ray AD, Bristow AWT (2011) Commentary: Challenging Convention Using Ambient Ionization and Direct Analysis Mass Spectrometric Techniques. *Rapid Commun Mass Spectrom* 25:821–825. doi:[10.1002/rcm.4925](https://doi.org/10.1002/rcm.4925)

8. Gross JH (2014) Direct Analysis in Real Time - A Critical Review of DART-MS. *Anal Bioanal Chem* 406:63–80. doi:[10.1007/s00216-013-7316-0](https://doi.org/10.1007/s00216-013-7316-0)
9. Hajslova J, Cajka T, Vavricka L (2011) Challenging Applications Offered by Direct Analysis in Real Time (DART) in Food-Quality and Safety Analysis. *Trends Anal Chem* 30:204–218. doi:[10.1016/j.trac.2010.11.001](https://doi.org/10.1016/j.trac.2010.11.001)
10. Haddad R, Sparrapan R, Eberlin MN (2006) Desorption Sonic Spray Ionization for (High) Voltage-Free Ambient Mass Spectrometry. *Rapid Commun Mass Spectrom* 20:2901–2905. doi:[10.1002/rcm.2680](https://doi.org/10.1002/rcm.2680)
11. Haddad R, Sparrapan R, Kotiaho T, Eberlin MN (2008) Easy ambient sonic-spray ionization-membrane interface Easy Ambient Sonic-Spray Ionization-Membrane Interface Mass Spectrometry for Direct Analysis of Solution Constituents. *Anal Chem* 80:898–903. doi:[10.1021/ac701960q](https://doi.org/10.1021/ac701960q)
12. Chen H, Zenobi R (2007) Direct Analysis of Living Objects by Extractive Electrospray Mass Ionization Spectrometry. *Chimia* 61:843. doi:[10.2533/chimia.2007.843](https://doi.org/10.2533/chimia.2007.843)
13. Chen H, Yang S, Wortmann A, Zenobi R (2007) Neutral Desorption Sampling of Living Objects for Rapid Analysis by Extractive Electrospray Ionization Mass Spectrometry. *Angew Chem Int Ed* 46:7591–7594. doi:[10.1002/anie.200702200](https://doi.org/10.1002/anie.200702200)
14. Takats Z, Cotte-Rodriguez I, Talaty N, Chen H, Cooks RG (2005) Direct, Trace Level Detection of Explosives on Ambient Surfaces by Desorption Electrospray Ionization Mass Spectrometry. *Chem Commun*:1950–1952. doi:[10.1039/B418697D](https://doi.org/10.1039/B418697D)
15. Williams JP, Patel VJ, Holland R, Scrivens JH (2006) The Use of Recently Described Ionisation Techniques for the Rapid Analysis of Some Common Drugs and Samples of Biological Origin. *Rapid Commun Mass Spectrom* 20:1447–1456. doi:[10.1002/rcm.2470](https://doi.org/10.1002/rcm.2470)
16. Haapala M, Pol J, Saarela V, Arvola V, Kotiaho T, Ketola RA, Franssila S, Kauppila TJ, Kostianen R (2007) Desorption Atmospheric Pressure Photoionization. *Anal Chem* 79:7867–7872. doi:[10.1021/ac071152g](https://doi.org/10.1021/ac071152g)
17. Cooks RG, Ouyang Z, Takats Z, Wiseman JM (2006) Ambient Mass Spectrometry. *Science* 311:1566–1570. doi:[10.1126/science.1119426](https://doi.org/10.1126/science.1119426)
18. Wells JM, Roth MJ, Keil AD, Grossenbacher JW, Justes DR, Patterson GE, Barket DJ (2008) Implementation of DART and DESI Ionization on a Fieldable Mass Spectrometer. *J Am Soc Mass Spectrom* 19:1419–1424. doi:[10.1016/j.jasms.2008.06.028](https://doi.org/10.1016/j.jasms.2008.06.028)
19. Takats Z, Wiseman JM, Gologan B, Cooks RG (2004) Electrosonic Spray Ionization. A Gentle Technique for Generating Folded Proteins and Protein Complexes in the Gas Phase and for Studying Ion-Molecule Reactions at Atmospheric Pressure. *Anal Chem* 76:4050–4058. doi:[10.1021/ac049848m](https://doi.org/10.1021/ac049848m)
20. Chen H, Talaty NN, Takats Z, Cooks RG (2005) Desorption Electrospray Ionization Mass Spectrometry for High-Throughput Analysis of Pharmaceutical Samples in the Ambient Environment. *Anal Chem* 77:6915–6927. doi:[10.1021/ac050989d](https://doi.org/10.1021/ac050989d)
21. Cotte-Rodriguez I, Takats Z, Talaty N, Chen H, Cooks RG (2005) Desorption Electrospray Ionization of Explosives on Surfaces: Sensitivity and Selectivity Enhancement by Reactive Desorption Electrospray Ionization. *Anal Chem* 77:6755–6764. doi:[10.1021/ac050995+](https://doi.org/10.1021/ac050995+)
22. Talaty N, Takats Z, Cooks RG (2005) Rapid in Situ Detection of Alkaloids in Plant Tissue Under Ambient Conditions Using Desorption Electrospray Ionization. *Analyst* 130:1624–1633. doi:[10.1039/B511161G](https://doi.org/10.1039/B511161G)
23. Dole RB (ed) (1997) *Electrospray Ionization Mass Spectrometry – Fundamentals, Instrumentation and Applications*. Wiley, Chichester
24. Pramanik BN, Ganguly AK, Gross ML (eds) (2002) *Applied Electrospray Mass Spectrometry*. Marcel Dekker, New York
25. Denes J, Katona M, Hosszu A, Czuczay N, Takats Z (2009) Analysis of Biological Fluids by Direct Combination of Solid Phase Extraction and Desorption Electrospray Ionization Mass Spectrometry. *Anal Chem* 81:1669–1675. doi:[10.1021/ac8024812](https://doi.org/10.1021/ac8024812)
26. Drayß M (2005) *Oberflächenanalytik mittels Desorptions Elektrospray Ionisation an einem Tripelquadrupolmassenspektrometer*. Heidelberg University, Dissertation

27. Takats Z, Kobliha V, Sevcik K, Novak P, Kruppa G, Lemr K, Havlicek V (2008) Characterization of DESI-FTICR Mass Spectrometry – From ECD to Accurate Mass Tissue Analysis. *J Mass Spectrom* 43:196–203. doi:[10.1002/jms.1285](https://doi.org/10.1002/jms.1285)
28. Hopf C, Schlueter M, Schwarz-Selinger T, von Toussaint U, Jacob W (2008) Chemical Sputtering of Carbon Films by Simultaneous Irradiation with Argon Ions and Molecular Oxygen. *New J Phys* 10:093022. doi:[10.1088/1367-2630/10/9/093022](https://doi.org/10.1088/1367-2630/10/9/093022)
29. Wiseman JM, Puolitaival SM, Takats Z, Cooks RG, Caprioli RM (2005) Mass Spectrometric Profiling of Intact Biological Tissue by Using Desorption Electrospray Ionization. *Angew Chem Int Ed* 44:7094–7097. doi:[10.1002/anie.200502362](https://doi.org/10.1002/anie.200502362)
30. Cotte-Rodriguez I, Hernandez-Soto H, Chen H, Cooks RG (2008) In Situ Trace Detection of Peroxide Explosives by Desorption Electrospray Ionization and Desorption Atmospheric Pressure Chemical Ionization. *Anal Chem* 80:1512–1519. doi:[10.1021/ac7020085](https://doi.org/10.1021/ac7020085)
31. Cotte-Rodriguez I, Mulligan CC, Cooks RG (2007) Non-Proximate Detection of Small and Large Molecules by Desorption Electrospray Ionization and Desorption Atmospheric Pressure Chemical Ionization Mass Spectrometry: Instrumentation and Applications in Forensics, Chemistry, and Biology. *Anal Chem* 79:7069–7077. doi:[10.1021/ac0707939](https://doi.org/10.1021/ac0707939)
32. Van Berkel GJ, Ford MJ, Deibel MA (2005) Thin-Layer Chromatography and Mass Spectrometry Coupled Using Desorption Electrospray Ionization. *Anal Chem* 77:1207–1215. doi:[10.1021/ac048217p](https://doi.org/10.1021/ac048217p)
33. Chen H, Zheng J, Zhang X, Luo M, Wang Z, Qiao X (2007) Surface Desorption Atmospheric Pressure Chemical Ionization Mass Spectrometry for Direct Ambient Sample Analysis Without Toxic Chemical Contamination. *J Mass Spectrom* 42:1045–1056. doi:[10.1002/jms.1235](https://doi.org/10.1002/jms.1235)
34. Chen H, Liang H, Ding J, Lai J, Huan Y, Qiao X (2007) Rapid Differentiation of Tea Products by Surface Desorption Atmospheric Pressure Chemical Ionization Mass Spectrometry. *J Agric Food Chem* 55:10093–10100. doi:[10.1021/jf0720234](https://doi.org/10.1021/jf0720234)
35. Yang S, Ding J, Zheng J, Hu B, Li J, Chen H, Zhou Z, Qiao X (2009) Detection of Melamine in Milk Products by Surface Desorption Atmospheric Pressure Chemical Ionization Mass Spectrometry. *Anal Chem* 81:2426–2436. doi:[10.1021/ac900063u](https://doi.org/10.1021/ac900063u)
36. Luosujarvi L, Arvola V, Haapala M, Pol J, Saarela V, Franssila S, Kotiaho T, Kostiainen R, Kauppila TJ (2008) Desorption and Ionization Mechanisms in Desorption Atmospheric Pressure Photoionization. *Anal Chem* 80:7460–7466. doi:[10.1021/ac801186x](https://doi.org/10.1021/ac801186x)
37. Luosujarvi L, Laakkonen UM, Kostiainen R, Kotiaho T, Kauppila TJ (2009) Analysis of Street Market Confiscated Drugs by Desorption Atmospheric Pressure Photoionization and Desorption Electrospray Ionization Coupled with Mass Spectrometry. *Rapid Commun Mass Spectrom* 23:1401–1404. doi:[10.1002/rcm.4005](https://doi.org/10.1002/rcm.4005)
38. Kauppila TJ, Arvola V, Haapala M, Pol J, Aalberg L, Saarela V, Franssila S, Kotiaho T, Kostiainen R (2008) Direct Analysis of Illicit Drugs by Desorption Atmospheric Pressure Photoionization. *Rapid Commun Mass Spectrom* 22:979–985. doi:[10.1002/rcm.3461](https://doi.org/10.1002/rcm.3461)
39. Hirabayashi Y, Takada Y, Hirabayashi A, Sakairi M, Koizumi H (1996) Direct Coupling of Semi-Micro Liquid Chromatography and Sonic Spray Ionization Mass Spectrometry for Pesticide Analysis. *Rapid Commun Mass Spectrom* 10:1891–1893. doi:[10.1002/\(SICI\)1097-0231\(199612\)10:15<1891::AID-RCM722>3.0.CO;2-R](https://doi.org/10.1002/(SICI)1097-0231(199612)10:15<1891::AID-RCM722>3.0.CO;2-R)
40. Hiraoka K (1996) Sonic Spray Ionization Mass Spectrometry. *J Mass Spectrom Soc Jpn* 44:279–284. doi:[10.5702/massspec.44.577](https://doi.org/10.5702/massspec.44.577)
41. Hirabayashi A, Fernandez de la Mora J (1998) Charged Droplet Formation in Sonic Spray. *Int J Mass Spectrom Ion Proc* 175:277–282. doi:[10.1016/S0168-1176\(98\)00129-3](https://doi.org/10.1016/S0168-1176(98)00129-3)
42. Haddad R, Catharino RR, Marques LA, Eberlin MN (2008) Perfume Fingerprinting by Easy Ambient Sonic-Spray Ionization Mass Spectrometry: Nearly Instantaneous Typification and Counterfeit Detection. *Rapid Commun Mass Spectrom* 22:3662–3666. doi:[10.1002/rcm.3788](https://doi.org/10.1002/rcm.3788)

43. Abdelnur PV, Eberlin LS, de Sa GF, de Souza V, Eberlin MN (2008) Single-Shot Biodiesel Analysis: Nearly Instantaneous Typification and Quality Control Solely by Ambient Mass Spectrometry. *Anal Chem* 80:7882–7886. doi:[10.1021/ac8014005](https://doi.org/10.1021/ac8014005)
44. Saraiva SA, Abdelnur PV, Catharino RR, Nunes G, Eberlin MN (2009) Fabric Softeners: Nearly Instantaneous Characterization and Quality Control of Cationic Surfactants by Easy Ambient Sonic-Spray Ionization Mass Spectrometry. *Rapid Commun Mass Spectrom* 23:357–362. doi:[10.1002/rcm.3878](https://doi.org/10.1002/rcm.3878)
45. Haddad R, Milagre HMS, Catharino RR, Eberlin MN (2008) Easy Ambient Sonic-Spray Ionization Mass Spectrometry Combined with Thin-Layer Chromatography. *Anal Chem* 80:2744–2750. doi:[10.1021/ac702216q](https://doi.org/10.1021/ac702216q)
46. Chen H, Venter A, Cooks RG (2006) Extractive Electrospray Ionization for Direct Analysis of Undiluted Urine, Milk and Other Complex Mixtures Without Sample Preparation. *Chem Commun*:2042–2044. doi:[10.1039/B602614A](https://doi.org/10.1039/B602614A)
47. Chen H, Wortmann A, Zenobi R (2007) Neutral Desorption Sampling Coupled to Extractive Electrospray Ionization Mass Spectrometry for Rapid Differentiation of Biosamples by Metabolomic Fingerprinting. *J Mass Spectrom* 42:1123–1135. doi:[10.1002/jms.1282](https://doi.org/10.1002/jms.1282)
48. Chang DY, Lee CC, Shiea J (2002) Detecting Large Biomolecules from High-Salt Solutions by Fused-Droplet Electrospray Ionization Mass Spectrometry. *Anal Chem* 74:2465–2469. doi:[10.1021/ac010788j](https://doi.org/10.1021/ac010788j)
49. Shieh IF, Lee CY, Shiea J (2005) Eliminating the Interferences from TRIS Buffer and SDS in Protein Analysis by Fused-Droplet Electrospray Ionization Mass Spectrometry. *J Proteome Res* 4:606–612. doi:[10.1021/pr049765m](https://doi.org/10.1021/pr049765m)
50. Chen H, Sun Y, Wortmann A, Gu H, Zenobi R (2007) Differentiation of Maturity and Quality of Fruit Using Noninvasive Extractive Electrospray Ionization Quadrupole Time-of-Flight Mass Spectrometry. *Anal Chem* 79:1447–1455. doi:[10.1021/ac061843x](https://doi.org/10.1021/ac061843x)
51. Chingin K, Gamez G, Chen H, Zhu L, Zenobi R (2008) Rapid Classification of Perfumes by Extractive Electrospray Ionization Mass Spectrometry (EESI-MS). *Rapid Commun Mass Spectrom* 22:2009–2014. doi:[10.1002/rcm.3584](https://doi.org/10.1002/rcm.3584)
52. Zhu L, Gamez G, Chen H, Chingin K, Zenobi R (2009) Rapid Detection of Melamine in Untreated Milk and Wheat Gluten by Ultrasound-Assisted Extractive Electrospray Ionization Mass Spectrometry (EESI-MS). *Chem Commun*:559–561. doi:[10.1039/B818541G](https://doi.org/10.1039/B818541G)
53. Chen H, Hu B, Hu Y, Huan Y, Zhou Z, Qiao X (2009) Neutral Desorption Using a Sealed Enclosure to Sample Explosives on Human Skin for Rapid Detection by EESI-MS. *J Am Soc Mass Spectrom* 20:719–722. doi:[10.1016/j.jasms.2008.12.011](https://doi.org/10.1016/j.jasms.2008.12.011)
54. Quist AP, Huth-Fehre T, Sundqvist BUR (1994) Total Yield Measurements in Matrix-Assisted Laser Desorption Using a Quartz Crystal Microbalance. *Rapid Commun Mass Spectrom* 8:149–154. doi:[10.1002/rcm.1290080204](https://doi.org/10.1002/rcm.1290080204)
55. Shiea J, Huang MZ, Hsu HJ, Lee CY, Yuan CH, Beech I, Sunner J (2005) Electrospray-Assisted Laser Desorption/Ionization Mass Spectrometry for Direct Ambient Analysis of Solids. *Rapid Commun Mass Spectrom* 19:3701–3704. doi:[10.1002/rcm.2243](https://doi.org/10.1002/rcm.2243)
56. Peng IX, Shiea J, Loo RRO, Loo JA (2007) Electrospray-Assisted Laser Desorption/Ionization and Tandem Mass Spectrometry of Peptides and Proteins. *Rapid Commun Mass Spectrom* 21:2541–2546. doi:[10.1002/rcm.3154](https://doi.org/10.1002/rcm.3154)
57. Huang MZ, Hsu HJ, Lee JY, Jeng J, Shiea J (2006) Direct Protein Detection from Biological Media Through Electrospray-Assisted Laser Desorption Ionization/Mass Spectrometry. *J Proteome Res* 5:1107–1116. doi:[10.1021/pr050442f](https://doi.org/10.1021/pr050442f)
58. Huang MZ, Hsu HJ, Wu CI, Lin SY, Ma YL, Cheng TL, Shiea J (2007) Characterization of the Chemical Components on the Surface of Different Solids with Electrospray-Assisted Laser Desorption Ionization Mass Spectrometry. *Rapid Commun Mass Spectrom* 21:1767–1775. doi:[10.1002/rcm.3011](https://doi.org/10.1002/rcm.3011)
59. Lin SY, Huang MZ, Chang HC, Shiea J (2007) Using Electrospray-Assisted Laser Desorption/Ionization Mass Spectrometry to Characterize Organic Compounds Separated on Thin-Layer Chromatography Plates. *Anal Chem* 79:8789–8795. doi:[10.1021/ac070590k](https://doi.org/10.1021/ac070590k)

60. Sampson JS, Hawkrigde AM, Muddiman DC (2006) Generation and Detection of Multiply-Charged Peptides and Proteins by Matrix-Assisted Laser Desorption Electrospray Ionization (MALDESI) Fourier Transform Ion Cyclotron Resonance Mass Spectrometry. *J Am Soc Mass Spectrom* 17:1712–1716. doi:[10.1016/j.jasms.2006.08.003](https://doi.org/10.1016/j.jasms.2006.08.003)
61. Nemes P, Vertes A (2007) Laser Ablation Electrospray Ionization for Atmospheric Pressure, In Vivo, and Imaging Mass Spectrometry. *Anal Chem* 79:8098–8106. doi:[10.1021/ac071181r](https://doi.org/10.1021/ac071181r)
62. Nemes P, Barton AA, Li Y, Vertes A (2008) Ambient Molecular Imaging and Depth Profiling of Live Tissue by Infrared Laser Ablation Electrospray Ionization Mass Spectrometry. *Anal Chem* 80:4575–4582. doi:[10.1021/ac8004082](https://doi.org/10.1021/ac8004082)
63. Sripadi P, Nazarian J, Hathout Y, Hoffman EP, Vertes A (2009) In Vitro Analysis of Metabolites from the Untreated Tissue of Torpedo Californica Electric Organ by Mid-Infrared Laser Ablation Electrospray Ionization Mass Spectrometry. *Metabolomics* 5:263–276. doi:[10.1007/s11306-008-0147-x](https://doi.org/10.1007/s11306-008-0147-x)
64. Bolt F, Cameron SJS, Karancsi T, Simon D, Schaffer R, Rickards T, Hardiman K, Burke A, Bodai Z, Perdones-Montero A, Rebec M, Balog J, Takats Z (2016) Automated High-Throughput Identification and Characterization of Clinically Important Bacteria and Fungi Using Rapid Evaporative Ionization Mass Spectrometry. *Anal Chem* 88:9419–9426. doi:[10.1021/acs.analchem.6b01016](https://doi.org/10.1021/acs.analchem.6b01016)
65. Balog J, Szaniszló T, Schaefer KC, Denes J, Lopata A, Godorhazy L, Szalay D, Balogh L, Sasi-Szabo L, Toth M, Takats Z (2010) Identification of Biological Tissues by Rapid Evaporative Ionization Mass Spectrometry. *Anal Chem* 82:7343–7350. doi:[10.1021/ac101283x](https://doi.org/10.1021/ac101283x)
66. Balog J, Kumar S, Alexander J, Golf O, Huang J, Wiggins T, Abbassi-Ghadi N, Enyedi A, Kacska S, Kinross J, Hanna GB, Nicholson JK, Takats Z (2015) In Vivo Endoscopic Tissue Identification by Rapid Evaporative Ionization Mass Spectrometry (REIMS). *Angew Chem Int Ed* 54:11059–11062. doi:[10.1002/anie.201502770](https://doi.org/10.1002/anie.201502770)
67. Strittmatter N, Rebec M, Jones EA, Golf O, Abdolrasouli A, Balog J, Behrends V, Veselkov KA, Takats Z (2014) Characterization and Identification of Clinically Relevant Microorganisms Using Rapid Evaporative Ionization Mass Spectrometry. *Anal Chem* 86:6555–6562. doi:[10.1021/ac501075f](https://doi.org/10.1021/ac501075f)
68. Golf O, Strittmatter N, Karancsi T, Pringle SD, Speller AVM, Mroz A, Kinross JM, Abbassi-Ghadi N, Jones EA, Takats Z (2015) Rapid Evaporative Ionization Mass Spectrometry Imaging Platform for Direct Mapping from Bulk Tissue and Bacterial Growth Media. *Anal Chem* 87:2527–2534. doi:[10.1021/ac5046752](https://doi.org/10.1021/ac5046752)
69. Balog J, Perenyi D, Guallar-Hoyas C, Egri A, Pringle SD, Stead S, Chevallier OP, Elliott CT, Takats Z (2016) Identification of the Species of Origin for Meat Products by Rapid Evaporative Ionization Mass Spectrometry. *J Agric Food Chem* 64:4793–4800. doi:[10.1021/acs.jafc.6b01041](https://doi.org/10.1021/acs.jafc.6b01041)
70. McEwen CN, McKay RG, Larsen BS (2005) Analysis of Solids, Liquids, and Biological Tissues Using Solids Probe Introduction at Atmospheric Pressure on Commercial LC/MS Instruments. *Anal Chem* 77:7826–7831. doi:[10.1021/ac051470k](https://doi.org/10.1021/ac051470k)
71. McEwen C, Gutteridge S (2007) Analysis of the Inhibition of the Ergosterol Pathway in Fungi Using the Atmospheric Solids Analysis Probe (ASAP) Method. *J Am Soc Mass Spectrom* 18:1274–1278. doi:[10.1016/j.jasms.2007.03.032](https://doi.org/10.1016/j.jasms.2007.03.032)
72. Smith MJP, Cameron NR, Mosely JA (2012) Evaluating Atmospheric Pressure Solids Analysis Probe (ASAP) Mass Spectrometry for the Analysis of Low Molecular Weight Synthetic Polymers. *Analyst* 137:4524–4530. doi:[10.1039/C2AN35556F](https://doi.org/10.1039/C2AN35556F)
73. Rozenski J (2011) Analysis of Nucleosides Using the Atmospheric-Pressure Solids Analysis Probe for Ionization. *Int J Mass Spectrom* 304:204–208. doi:[10.1016/j.ijms.2011.01.029](https://doi.org/10.1016/j.ijms.2011.01.029)
74. Driffield M, Bradley E, Castle L, Lloyd A, Parmar M, Speck D, Roberts D, Stead S (2015) Use of Atmospheric Pressure Solids Analysis Probe Time-of-Flight Mass Spectrometry to

- Screen for Plasticisers in Gaskets Used in Contact with Foods. *Rapid Commun Mass Spectrom* 29:1603–1610. doi:[10.1002/rcm.7255](https://doi.org/10.1002/rcm.7255)
75. Doue M, Dervilly-Pinel G, Gicquiau A, Pouponneau K, Monteau F, Le Bizet B (2014) High Throughput Identification and Quantification of Anabolic Steroid Esters by Atmospheric Solids Analysis Probe Mass Spectrometry for Efficient Screening of Drug Preparations. *Anal Chem* 86:5649–5655. doi:[10.1021/ac501072g](https://doi.org/10.1021/ac501072g)
76. Pan H, Lundin G (2011) Rapid Detection and Identification of Impurities in Ten 2-Naphthalenamines Using an Atmospheric Pressure Solids Analysis Probe in Conjunction with Ion Mobility Mass Spectrometry. *Eur J Mass Spectrom* 17:217–225. doi:[10.1255/ejms.1125](https://doi.org/10.1255/ejms.1125)
77. Kusai A (2007) Fundamental and Application of the Direct Analysis in Real Time Mass Spectrometry. *Bunseki* 124–127
78. Saitoh K (2007) Directly Analysis for Fragrance Ingredients Using DART-TOFMS. *Aroma Res* 8:366–369
79. Sparkman OD, Jones PR, Curtis M (2009) Accurate mass measurements with a reflectron time-of-flight mass spectrometer and the direct analysis in real time (DART) interface for the identification of unknown compounds below masses of 500 DA. In: Li L (ed) *Chemical Analysis*. Wiley, Hoboken
80. Konuma K (2009) Elementary Guide to Ionization Methods for Mass Spectrometry: Introduction of the Direct Analysis in Real Time Mass Spectrometry. *Bunseki* 464–467
81. Chernetsova ES, Bochkov PO, Ovcharov MV, Zhokhov SS, Abramovich RA (2010) DART Mass Spectrometry: A Fast Screening of Solid Pharmaceuticals for the Presence of an Active Ingredient, As an Alternative for IR Spectroscopy. *Drug Test Anal* 2:292–294. doi:[10.1002/dta.136](https://doi.org/10.1002/dta.136)
82. Kikura-Hanajiri R (2010) Simple and Rapid Screening for Target Compounds Using Direct Analysis in Real Time (DART)-MS. *Food Food Ingredients Jpn* 215:137–143
83. Chernetsova ES, Morlock GE (2011) Mass Spectrometric Method of Direct Sample Analysis in Real Time (DART) and Application of the Method to Pharmaceutical and Biological Analysis. *Zavodskaya Laboratoriya, Diagnostika Materialov* 77:10–19
84. Chernetsova ES, Morlock GE, Revelsky IA (2011) DART Mass Spectrometry and Its Applications in Chemical Analysis. *Russ Chem Rev* 80:235–255. doi:[10.1070/RC2011v080n03ABEH0004194](https://doi.org/10.1070/RC2011v080n03ABEH0004194)
85. Chernetsova ES, Morlock GE (2011) Determination of Drugs and Drug-Like Compounds in Different Samples with Direct Analysis in Real Time Mass Spectrometry. *Mass Spectrom Rev* 30:875–883. doi:[10.1002/mas.20304](https://doi.org/10.1002/mas.20304)
86. Liao J, Liu N, Liu C (2011) Direct Analysis in Real Time Mass Spectrometry and Its Applications to Drug Analysis. *Yaowu Fenxi Zazhi* 31:2008–2012
87. Osuga J, Konuma K (2011) Applications of Direct Analysis in Real Time (DART) Mass Spectrometry. *Yuki Gosei Kagaku Kyokaishi* 69:171–175. doi:[10.5059/yukigoseikyokaishi.69.171](https://doi.org/10.5059/yukigoseikyokaishi.69.171)
88. Shelley JT, Wiley JS, Chan GCY, Schilling GD, Ray SJ, Hieftje GM (2009) Characterization of Direct-Current Atmospheric-Pressure Discharges Useful for Ambient Desorption/Ionization Mass Spectrometry. *J Am Soc Mass Spectrom* 20:837–844. doi:[10.1016/j.jasms.2008.12.020](https://doi.org/10.1016/j.jasms.2008.12.020)
89. Andrade FJ, Shelley JT, Wetzel WC, Webb MR, Gamez G, Ray SJ, Hieftje GM (2008) Atmospheric Pressure Chemical Ionization Source. 1. Ionization of Compounds in the Gas Phase. *Anal Chem* 80:2646–2653. doi:[10.1021/ac800156y](https://doi.org/10.1021/ac800156y)
90. Andrade FJ, Shelley JT, Wetzel WC, Webb MR, Gamez G, Ray SJ, Hieftje GM (2008) Atmospheric Pressure Chemical Ionization Source. 2. Desorption-Ionization for the Direct Analysis of Solid Compounds. *Anal Chem* 80:2654–2663. doi:[10.1021/ac800210s](https://doi.org/10.1021/ac800210s)
91. Warscheid B, Hoffmann T (2001) Structural Elucidation of Monoterpene Oxidation Products by Ion Trap Fragmentation Using on-Line Atmospheric Pressure Chemical Ionization Mass

- Spectrometry in the Negative Ion Mode. *Rapid Commun Mass Spectrom* 15:2259–2272. doi:[10.1002/rcm.504](https://doi.org/10.1002/rcm.504)
92. Song L, Dykstra AB, Yao H, Bartmess JE (2009) Ionization Mechanism of Negative Ion-Direct Analysis in Real Time: A Comparative Study with Negative Ion-Atmospheric Pressure Photoionization. *J Am Soc Mass Spectrom* 20:42–50. doi:[10.1016/j.jasms.2008.09.016](https://doi.org/10.1016/j.jasms.2008.09.016)
93. Derpmann V, Albrecht S, Benter T (2012) The Role of Ion-Bound Cluster Formation in Negative Ion Mass Spectrometry. *Rapid Commun Mass Spectrom* 26:1923–1933. doi:[10.1002/rcm.6303](https://doi.org/10.1002/rcm.6303)
94. Klee S, Derpmann V, Wissdorf W, Klopotoski S, Kersten H, Brockmann KJ, Benter T, Albrecht S, Bruins AP, Dousty F, Kauppila TJ, Kostiaainen R, O'Brien R, Robb DB, Syage JA (2014) Are Clusters Important in Understanding the Mechanisms in Atmospheric Pressure Ionization? Part 1: Reagent Ion Generation and Chemical Control of Ion Populations. *J Am Soc Mass Spectrom* 25:1310–1321. doi:[10.1007/s13361-014-0891-2](https://doi.org/10.1007/s13361-014-0891-2)
95. Cody RB (2009) Observation of Molecular Ions and Analysis of Nonpolar Compounds with the Direct Analysis in Real Time Ion Source. *Anal Chem* 81:1101–1107. doi:[10.1021/ac8022108](https://doi.org/10.1021/ac8022108)
96. Jorabchi K, Hanold K, Syage J (2013) Ambient Analysis by Thermal Desorption Atmospheric Pressure Photoionization. *Anal Bioanal Chem* 405:7011–7018. doi:[10.1007/s00216-012-6536-z](https://doi.org/10.1007/s00216-012-6536-z)
97. Rummel JL, McKenna AM, Marshall AG, Eyler JR, Powell DH (2010) The Coupling of Direct Analysis in Real Time Ionization to Fourier Transform Ion Cyclotron Resonance Mass Spectrometry for Ultrahigh-Resolution Mass Analysis. *Rapid Commun Mass Spectrom* 24:784–790. doi:[10.1002/rcm.4450](https://doi.org/10.1002/rcm.4450)
98. Dane AJ, Cody RB (2010) Selective Ionization of Melamine in Powdered Milk by Using Argon Direct Analysis in Real Time (DART) Mass Spectrometry. *Analyst* 135:696–699. doi:[10.1039/b923561b](https://doi.org/10.1039/b923561b)
99. Yang H, Wan D, Song F, Liu Z, Liu S (2013) Argon Direct Analysis in Real Time Mass Spectrometry in Conjunction with Makeup Solvents: A Method for Analysis of Labile Compounds. *Anal Chem* 85:1305–1309. doi:[10.1021/ac3026543](https://doi.org/10.1021/ac3026543)
100. Cody RB, Dane AJ (2013) Soft Ionization of Saturated Hydrocarbons, Alcohols and Nonpolar Compounds by Negative-Ion Direct Analysis in Real-Time Mass Spectrometry. *J Am Soc Mass Spectrom* 24:329–334. doi:[10.1007/s13361-012-0569-6](https://doi.org/10.1007/s13361-012-0569-6)
101. Harper JD, Charipar NA, Mulligan CC, Zhang X, Cooks RG, Ouyang Z (2008) Low-Temperature Plasma Probe for Ambient Desorption Ionization. *Anal Chem* 80:9097–9104. doi:[10.1021/ac801641a](https://doi.org/10.1021/ac801641a)
102. Tsuchiya M, Taira T (1978) A New Ionization Method for Organic Compounds. Liquid Ionization at Atmospheric Pressure Utilizing Penning Effect and Chemical Ionization. *Shitsuryo Bunseki* 26:333–342
103. Tsuchiya M, Taira T, Toyoura Y (1980) A New Ionization Detector for Minute Amounts of Organic Compounds in Solution. *Bunseki Kagaku* 29:632–637
104. McLuckey SA, Glish GL, Asano KG, Grant BC (1988) Atmospheric Sampling Glow Discharge Ionization Source for the Determination of Trace Organic Compounds in Ambient Air. *Anal Chem* 60:2220–2227. doi:[10.1021/ac00171a012](https://doi.org/10.1021/ac00171a012)
105. Fujimaki S, Furuya H, Kambara S, Hiraoka K (2004) Development of an Atmospheric Pressure Penning Ionization Source for Gas Analysis. *J Mass Spectrom Soc Jpn* 52:149–153. doi:[10.5702/massspec.52.149](https://doi.org/10.5702/massspec.52.149)
106. Hiraoka K, Fujimaki S, Kambara S, Furuya H, Okazaki S (2004) Atmospheric-Pressure Penning Ionization Mass Spectrometry. *Rapid Commun Mass Spectrom* 18:2323–2330. doi:[10.1002/rcm.1624](https://doi.org/10.1002/rcm.1624)
107. Furuya H, Kambara S, Nishidate K, Fujimaki S, Hashimoto Y, Suzuki S, Iwama T, Hiraoka K (2010) Quantitative Aspects of Atmospheric-Pressure Penning Ionization. *J Mass Spectrom Soc Jpn* 58:211–213. doi:[10.5702/massspec.58.211](https://doi.org/10.5702/massspec.58.211)

108. Ratcliffe LV, Rutten FJM, Barrett DA, Whitmore T, Seymour D, Greenwood C, Aranda-Gonzalvo Y, Robinson S, McCoustra M (2007) Surface Analysis Under Ambient Conditions Using Plasma-Assisted Desorption/Ionization Mass Spectrometry. *Anal Chem* 79:6094–6101. doi:[10.1021/ac070109q](https://doi.org/10.1021/ac070109q)
109. Na N, Zhao M, Zhang S, Yang C, Zhang X (2007) Development of a Dielectric Barrier Discharge Ion Source for Ambient Mass Spectrometry. *J Am Soc Mass Spectrom* 18:1859–1862. doi:[10.1016/j.jasms.2007.07.027](https://doi.org/10.1016/j.jasms.2007.07.027)
110. Na N, Zhang C, Zhao M, Zhang S, Yang C, Fang X, Zhang X (2007) Direct Detection of Explosives on Solid Surfaces by Mass Spectrometry with an Ambient Ion Source Based on Dielectric Barrier Discharge. *J Mass Spectrom* 42:1079–1085. doi:[10.1002/jms.1243](https://doi.org/10.1002/jms.1243)
111. Hiraoka K, Ninomiya S, Chen LC, Iwama T, Mandal MK, Suzuki H, Ariyada O, Furuya H, Takekawa K (2011) Development of Double Cylindrical Dielectric Barrier Discharge Ion Source. *Analyst* 136:1210–1215. doi:[10.1039/c0an00621a](https://doi.org/10.1039/c0an00621a)
112. Wetzel WC, Andrade FJ, Broekaert JAC, Hieftje GM (2006) Development of a Direct Current He Atmospheric-Pressure Glow Discharge as an Ionization Source for Elemental Mass Spectrometry Via Hydride Generation. *J Anal At Spectrom* 21:750–756. doi:[10.1039/b607781a](https://doi.org/10.1039/b607781a)
113. McEwen CN, Larsen BS (2009) Ionization Mechanisms Related to Negative Ion APPI, APCI, and DART. *J Am Soc Mass Spectrom* 20:1518–1521. doi:[10.1016/j.jasms.2009.04.010](https://doi.org/10.1016/j.jasms.2009.04.010)
114. Cristoni S, Bernardi LR, Biunno I, Tubaro M, Guidugli F (2003) Surface-Activated No-Discharge Atmospheric Pressure Chemical Ionization. *Rapid Commun Mass Spectrom* 17:1973–1981. doi:[10.1002/rcm.1141](https://doi.org/10.1002/rcm.1141)
115. Cristoni S, Bernardi LR, Guidugli F, Tubaro M, Traldi P (2005) The Role of Different Phenomena in Surface-Activated Chemical Ionization (SACI) Performance. *J Mass Spectrom* 40:1550–1557. doi:[10.1002/jms.913](https://doi.org/10.1002/jms.913)
116. Chen H, Ouyang Z, Cooks RG (2006) Thermal Production and Reactions of Organic Ions at Atmospheric Pressure. *Angew Chem Int Ed* 45:3656–3660. doi:[10.1002/anie.200600660](https://doi.org/10.1002/anie.200600660)
117. Perez JJ, Harris GA, Chipuk JE, Brodbelt JS, Green MD, Hampton CY, Fernandez FM (2010) Transmission-Mode Direct Analysis in Real Time and Desorption Electrospray Ionization Mass Spectrometry of Insecticide-Treated Bednets for Malaria Control. *Analyst* 135:712–719. doi:[10.1039/b924533b](https://doi.org/10.1039/b924533b)
118. Chernetsova ES, Revelsky AI, Morlock GE (2011) Some New Features of Direct Analysis in Real Time Mass Spectrometry Utilizing the Desorption at an Angle Option. *Rapid Commun Mass Spectrom* 25:2275–2282. doi:[10.1002/rcm.5112](https://doi.org/10.1002/rcm.5112)
119. Fernandez FM, Cody RB, Green MD, Hampton CY, McGready R, Sengaloundeth S, White NJ, Newton PN (2006) Characterization of Solid Counterfeit Drug Samples by Desorption Electrospray Ionization and Direct-Analysis-in-Real-Time Coupled to Time-of-Flight Mass Spectrometry. *ChemMedChem* 1:702–705. doi:[10.1002/cmdc.200600041](https://doi.org/10.1002/cmdc.200600041)
120. Jones RW, Cody RB, McClelland JF (2006) Differentiating Writing Inks Using Direct Analysis in Real Time Mass Spectrometry. *J Forensic Sci* 51:915–918. doi:[10.1111/j.1556-4029.2006.00162.x](https://doi.org/10.1111/j.1556-4029.2006.00162.x)
121. Yu S, Crawford E, Tice J, Musselman B, Wu JT (2009) Bioanalysis Without Sample Cleanup or Chromatography: The Evaluation and Initial Implementation of Direct Analysis in Real Time Ionization Mass Spectrometry for the Quantification of Drugs in Biological Matrixes. *Anal Chem* 81:193–202. doi:[10.1021/ac801734t](https://doi.org/10.1021/ac801734t)
122. Zhao Y, Lam M, Wu D, Mak R (2008) Quantification of Small Molecules in Plasma with Direct Analysis in Real Time Tandem Mass Spectrometry, Without Sample Preparation and Liquid Chromatographic Separation. *Rapid Commun Mass Spectrom* 22:3217–3224. doi:[10.1002/rcm.3726](https://doi.org/10.1002/rcm.3726)
123. Jagerdeo E, Abdel-Rehim M (2009) Screening of Cocaine and Its Metabolites in Human Urine Samples by Direct Analysis in Real-Time Source Coupled to Time-of-Flight Mass

- Spectrometry After Online Preconcentration Utilizing Microextraction by Packed Sorbent. *J Am Soc Mass Spectrom* 20:891–899. doi:[10.1016/j.jasms.2009.01.010](https://doi.org/10.1016/j.jasms.2009.01.010)
124. Kpegba K, Spadaro T, Cody RB, Nesnas N, Olson JA (2007) Analysis of Self-Assembled Monolayers on Gold Surfaces Using Direct Analysis in Real Time Mass Spectrometry. *Anal Chem* 79:5479–5483. doi:[10.1021/ac062276g](https://doi.org/10.1021/ac062276g)
125. Block E, Dane AJ, Cody RB (2011) Crushing Garlic and Slicing Onions: Detection of Sulfenic Acids and Other Reactive Organosulfur Intermediates from Garlic and Other Alliums Using Direct Analysis in Real-Time Mass Spectrometry (DART-MS). *Phosphorus Sulfur Silicon Rel Elem* 186:1085–1093. doi:[10.1080/10426507.2010.507728](https://doi.org/10.1080/10426507.2010.507728)
126. Block E, Dane AJ, Thomas S, Cody RB (2010) Applications of Direct Analysis in Real Time Mass Spectrometry (DART-MS) in Allium Chemistry. 2-Propenesulfenic and 2-Propenesulfinic Acids, Diallyl trisulfane S-oxide, and Other Reactive Sulfur Compounds from Crushed Garlic and Other Alliums. *J Agric Food Chem* 58:4617–4625. doi:[10.1021/jf1000106](https://doi.org/10.1021/jf1000106)
127. Yew JY, Cody RB, Kravitz EA (2008) Cuticular Hydrocarbon Analysis of an Awake Behaving Fly Using Direct Analysis in Real-Time Time-of-Flight Mass Spectrometry. *Proc Natl Acad Sci U S A* 105:7135–7140. doi:[10.1073/pnas.0802692105](https://doi.org/10.1073/pnas.0802692105)
128. Gross JH (2013) Polydimethylsiloxane-Based Wide Range Mass Calibration for Direct Analysis in Real Time Mass Spectrometry. *Anal Bioanal Chem* 405:8663–8668. doi:[10.1007/s00216-013-7287-1](https://doi.org/10.1007/s00216-013-7287-1)
129. Gross JH (2015) Analysis of Silicones Released from Household Items and Baby Articles by Direct Analysis in Real Time-Mass Spectrometry. *J Am Soc Mass Spectrom* 26:511–521. doi:[10.1007/s13361-014-1042-5](https://doi.org/10.1007/s13361-014-1042-5)
130. Gross JH (2015) Direct Analysis in Real Time Mass Spectrometry and Its Application for the Analysis of Polydimethylsiloxanes. *Spectrosc Eur* 27:6–11
131. Gross JH (2015) Polydimethylsiloxane Extraction from Silicone Rubber into Baked Goods Detected by Direct Analysis in Real Time Mass Spectrometry. *Eur J Mass Spectrom* 21:313–319. doi:[10.1255/ejms.1333](https://doi.org/10.1255/ejms.1333)
132. Jakob A, Crawford EA, Gross JH (2016) Detection of Polydimethylsiloxanes Transferred from Silicone-Coated Parchment Paper to Baked Goods Using Direct Analysis in Real Time Mass Spectrometry. *J Mass Spectrom* 51:298–304. doi:[10.1002/jms.3757](https://doi.org/10.1002/jms.3757)

<http://www.springer.com/978-3-319-54397-0>

Mass Spectrometry

A Textbook

Gross, J.H.

2017, XXV, 968 p. 664 illus., 201 illus. in color.,

Hardcover

ISBN: 978-3-319-54397-0